Zentrum für Technomathematik
Fachbereich 3 – Mathematik und Informatik

Modelling and simulation of concrete carbonation: competition of several carbonation reactions

Malte A. Peter, Adrian Muntean,
Sebastian A. Meier, Michael Böhm

Report 05–03

Berichte aus der Technomathematik

Report 05–03 April 2005

Modelling and simulation of concrete carbonation: competition of several carbonation reactions

Malte A. Peter, Adrian Muntean, Sebastian A. Meier, Michael Böhm

Centre for Industrial Mathematics, FB 3, University of Bremen, Germany
e-mails: {mpeter,muntean,sebam,mbohm}@math.uni-bremen.de

Abstract

Concrete carbonation, i.e. the reaction of alkaline species (inside the concrete) with atmospheric carbon dioxide, is one of the major physicochemical processes compromising the service life of concrete structures. While the main carbonation reaction is that of calcium hydroxide, other constituents such as calcium silicates or calcium-silcate hydrates in the concrete can also carbonate. Many authors neglect the carbonation of these additional constituents competing with calcium hydroxide for carbon dioxide when formulating prediction models. This paper is concerned with the theoretical and numerical investigation of this competition. In particular, the effect on the simulated carbonation depth, i.e. the depth how far the carbonation layer has advanced into the concrete at any given time, is investigated. For this purpose, the concrete-carbonation process is modelled by a semi-linear coupled system of reaction-diffusion equations. For this system, a dimensional analysis is carried out and it is solved by numerical techniques. Experimental data is used for reference.

Key words: Reaction-diffusion systems, concrete carbonation, fast reactions, Thiele modulus, internal layers

Contents

1 Introduction

Steel bars in reinforced concrete are protected from corrosion by the highly alkaline environment inside the concrete (pH $\approx$ 13). If the pH decreases in the environment of the reinforcements, this protection ceases and the steel bars can corrode. Consequently, the rusting of the reinforcement usually leads to a severe reduction of the durability of the structure. The main process that destroys the protection by alkalinity is concrete carbonation, i.e. the reaction of alkaline species (in the concrete) with atmospheric carbon dioxide to produce calcium carbonate amongst other species. Detailed surveys and literature accounts on the carbonation problem and related aspects concerning the durability of concrete can be found, for instance, in [Bie88, Kro95, Cha99, MIK03, Sis04] and references therein.

The carbonation process is associated with several reaction and transport mechanisms. The main carbonation reaction is that of calcium hydroxide which may be described by

$$\mathrm{CO_2}(g \to aq) + \mathrm{Ca(OH)_2}(s \to aq) \longrightarrow \mathrm{CaCO_3}(aq \to s) + \mathrm{H_2O}. \tag{1.1}$$

Other constituents in the concrete can also carbonate, particularly calcium-silicate hydrate (CSH) and unhydrated calcium silicates (CS), but are commonly neglected when simulating concrete carbonation. The main focus of this paper is the investigation of the influence of these (usually neglected) species and the effects of their competition with calcium hydroxide for carbon dioxide in concretes with ordinary portland cement (OPC).

A short summary of the carbonation scenario that we focus on here can be given as follows: The atmospheric carbon dioxide diffuses through the unsaturated concrete matrix, dissolves in the pore water via a Henry-like transfer mechanism, and then reacts in the presence of water with available carbonatable constituents. These are available in the pore solution by dissolution from the solid matrix. At the same time, CS hydrate (i.e. they react with water) to calcium hydroxide and CSH. Once building up, carbonates precipitate quickly to the solid matrix.

Experimental evidence suggests that the bulk of the carbonation reaction (1.1) is located on an internal *reaction layer* of a priori unknown width which is formed initially and progresses into the material afterwards [cf. PVF89, e.g.]. Therefore, our main interest is in the carbonation pentration depth, which determines how far this reaction layer has advanced into the concrete sample at a given time. It was also shown experimentally that the CSH starts carbonating as soon as the available calcium hydroxide has been depleted by via (1.1) [cf. Cha97, e.g.]. However, it is not clear when the carbonation of CS starts.

The carbonation reactions of the other carbonatable species are not as fast as that of calcium hydroxide but are still faster than the hydration reactions (in the late stage of hydration considered here). However, all of these reactions compete for carbon dioxide. It is the aim of this research to investigate the competition of carbonation and hydration as well as the competition between several parallel carbonation reactions. This is particularly interesting since many authors neglect all of these aspects when modelling and simulating concrete carbonation which may lead to an over-estimation of the real carbonation depth. We investigate the formation and the evolution of possible additional internal layers associated with the respective reactions of the other carbonatable constituents. This is particularly studied with respect to the layer formed due to the carbonation of calcium hydroxide. The numerical studies are based on a proper nondimensionalisation of the governing system of equations allowing easy comparisons and identification of characteristic time scales.

Cf. [Ram01, Tay97], e.g., there are various problems associated with the determination of water chemically associated with CSH. For instance, it is difficult to really distinguish this (gel) water from the free water which is present in the pores. In our model, we explicitly distinguish between the moisture (pore water and moist air) and the gel water and only consider the evolution of the moisture while assuming a constant (sufficient) amount of gel water to be present in the porous matrix. However, more research has to be initiated in order to translate the present considerations in a double-porosity model [cf. Hor97, e.g.] which might be more appropriate to describe such scenarios. Such a model allows for variations in the gel porosities as well. Evidence on concrete materials presenting a double-porosity structure has been drawn by Houst and Wittmann [cf. Hou96, HW02]. We do not strictly follow this direction here and rather try to see some of the effects due to the carbonation of CSH and unhydrated constituents on the penetration curve which is the main output of the model. This problem is also related to the various morphologies and multiple choice of stoichiometry for the CSH compound. In this work, the precise morphology and stoichiometry of CSH plays no role. For definiteness, we only consider one particular stoichiometry for CSH.

We consider the hydration process in its final period (namely, much time after the 26 hours after the mixing referred to in table 1 in [MS01], e.g.). In an accelerated test, it is usually *assumed* that the hydration is complete [cf. Sis04, Ste00]. Nevertheless, we account for an *almost complete* hydration reaction and study a special competition between hydration and carbonation of unhydrated constituents. We do not go into detail in what the modelling of the hydration is concerned but rather refer the reader to [Tay97, Ram01, PVF89] for fairly detailed descriptions of the physicochemical processes, or to [PBK01, SBK03] for a presentation of some mathematical issues concerning some of the existing hydration models.

The paper is organised as follows: In section 2, the problem under consideration is specified in detail and we particularly discuss the chemical processes associated with the concrete-carbonation problem. In section 3, these results are used to formulate a complete system of reaction-diffusion equations including intial and boundary conditions for all species under consideration. In order to investigate numerically the course of the carbonation process we introduce a weak formulation of the problem and perform its nondimensionalisation in section 4. The largest part of this paper is section 5. It contains a significant part of our numerical experiments. Basic results (penetration curves and concentration profiles) obtained when simulating an accelerated carbonation test are given. We particularly study the competition of carbonation and hydration and that between the different carbonation reactions as well as their effect on the penetration curves. Moreover, we investigate the effect of changes in the rapidness of the carbonation and hydration reactions on the penetration curves. Finally, we summarise the simulation results and conclusions in 6. The values of all parameters used in this paper can be found in the appendix.

2 Main setting

In this section we shortly describe the setting under consideration and discuss some chemical issues. Moreover, the basic geometry and notation is introduced.

2.1 Basic geometry and porosity

We focus on a part of a concrete member which is exposed to ingress of gaseous CO_2 and humidity from the environment. Fig. 1a shows a typical control volume (box A) in such a structure. We denote by Ω the part of the concrete sample contained in box A, for which we model the carbonation process. The dark area points out a zone $\Omega_\epsilon(t)$ or a very thin front $\Gamma(t)$ of steep change in pH dependent on the time variable t. This indicates that the carbonation reaction is in its fast regime: namely the characteristic reaction time is much faster than the characteristic diffusion time of the fastest active species (here $CO_2(g)$). $\Omega_2(t)$ denotes the *uncarbonated zone*, $\Omega_1(t)$ is the *carbonated zone*, and Γ^{N} and Γ^{R} are the interior and exterior boundaries, respectively (not shown in the figure). For ease of notation, we also define $\Gamma := \Gamma^{\mathrm{N}} \cup \Gamma^{\mathrm{R}}$. Our considerations are also valid for cylindrical concrete structures as long as the carbonation-reaction zone has not advanced too far into the concrete. Then, what we have in mind is depicted in Fig. 1b and Ω is the concrete part of box B. Since we are only interested in the forming and propagation of the carbonation layers within Ω, we do not consider situations where the layers get close to the unexposed boundary Γ^{N}. We prescribe homogeneous Neumann boundary conditions at these parts (cf. section 3). Therefore, the real width of the concrete sample is of no relevance in our considerations as long as Ω is chose wide enough. Unlike the case of moving-interface formulations [BKM03b, e.g.], we cannot say anything *a priori* about the widths of the carbonated and uncarbonated regions.

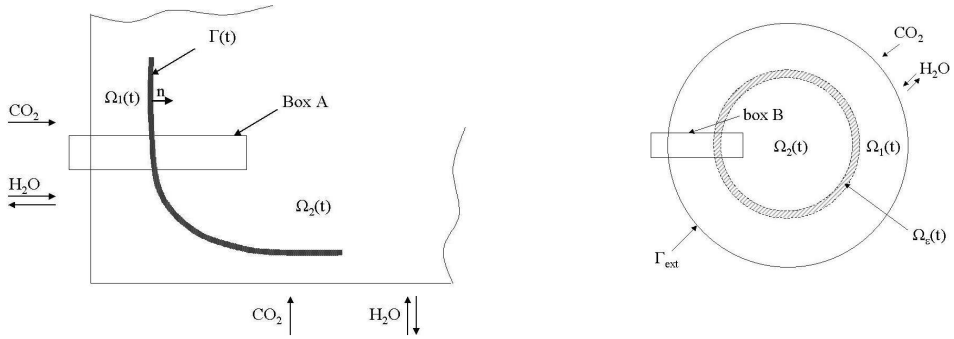

Figure 1: a) Typical corner of a concrete structure. Box A is the region which our model refers to. b) Cross section of a cylindrical concrete sample. Box B is the region which our model refers to.

We introduce some concepts usually needed to describe reactive processes taking place in porous media. Ω is composed of the solid matrix Ω^{s} and of the totality of pore voids Ω^{p}. Furthermore, since the pore space is unsaturated and carbonation is a heterogeneous process, Ω^{p} splits into Ω^{a} (the parts filled with dry air and water vapors) and Ω^{w}(the parts filled with liquid water). We denote by the volumetric ratio $\phi := |\Omega^{\mathrm{p}}|/|\Omega|$ the concrete porosity and by $\phi^j := |\Omega^j|/|\Omega^{\mathrm{p}}|$ the air and water fractions, where $j \in \{\mathrm{a}, \mathrm{w}\}$. Like other authors [cf. SSV95, SV04, Ste00, e.g.], we assume a constant concrete porosity, i.e. the porosity does not change during the course of carbonation and last stage of hydration. Cf. [PVF89], we calculate it as

$$\phi := \frac{R_{\mathrm{w/c}} \frac{\rho_{\mathrm{c}}}{\rho_{\mathrm{w}}}}{\left(R_{\mathrm{w/c}} \frac{\rho_{\mathrm{c}}}{\rho_{\mathrm{w}}} + R_{\mathrm{a/c}} \frac{\rho_{\mathrm{c}}}{\rho_{\mathrm{a}}} + 1 \right)}, \tag{2.1}$$

where $R_{w/c}$ and $R_{a/c}$ represent the water-to-cement and aggregate-to-cement ratios, while ρ_a, ρ_w and ρ_c are aggregate, water and concrete densities, respectively. Throughout the paper, the space variable is denoted by $x \in \Omega$.

2.2 Chemistry

It is well-known [cf. PVF89, e.g.] that if the hydration reactions are not complete, then some of the unhydrated constituents may carbonate. Consequently, we expect that a special competition between hydration and carbonation reactions may take place in the concrete structure. Such a competition does not seem to be too significant in the case of accelerated testing, mainly due to the high hydration degree which is reached by the sample during the period before the accelerated test starts. On the other hand, since much more CO_2 is available for reaction, the effect might be stronger yet again. For natural carbonation, these competitive effects might be stronger because of the lower (initial) degree of hydration of the sample [cf. Ste00, PVF89]. On the other hand, for a natural carbonation setting the state of hydration at a given time is generally unknown. For this reason, we focus on the simulation of accelerated tests for which the state of hydration is fairly certain at the beginning of the test. Nevertheless, the model derived in the sequel also applies to natural carbonation. The carbonation of other alkaline species like KOH, NaOH and $Mg(OH)_2$, e.g., and of the aluminate phases is neglected in this first approach. See [Ste00, e.g.] for more details on this subject.

2.2.1 Hydration reactions

The main species to be hydrated are $2CaO \cdot SiO_2$ (dicalcium silicate, C_2S) and $3CaO \cdot SiO_2$ (tricalcium silicate, C_3S). The products of their hydration are $3CaO \cdot 2SiO_2 \cdot 3H_2O$ (calcium silicate hydrate, CSH) and $Ca(OH)_2$. The hydration reactions of C_2S and C_3S are given by

$$2(2CaO \cdot SiO_2) + 4H_2O \longrightarrow (3CaO \cdot 2SiO_2 \cdot 3H_2O) + Ca(OH)_2, \tag{2.2}$$

$$2(3CaO \cdot SiO_2) + 6H_2O \longrightarrow (3CaO \cdot 2SiO_2 \cdot 3H_2O) + 3Ca(OH)_2, \tag{2.3}$$

respectively [cf. Tay97, PVF89, e.g.]. In the hydration reactions (2.2) and (2.3), water is consumed. However, these reactions take place in the (porous) matrix space (as opposed to the pore space) at the late stage of hydration considered here. By matrix space we mean the concrete matrix which can be considered a porous medium (of low permeability) itself [see Hor97, for some details concerning the notion of double-porosity models]. We assume that there is a sufficient amount of water available in the matrix space for the hydration reactions to be completed.

2.2.2 Carbonation reactions

The main carbonation reaction can be described by

$$Ca(OH)_2 + CO_2 \longrightarrow CaCO_3 + H_2O. \tag{2.4}$$

Beside $Ca(OH)_2$, the other hydration product CSH and as well as unhydrated constituents such as C_2S and C_3S are susceptible to carbonation. Their carbonation reactions can be described via

$$(3CaO \cdot 2SiO_2 \cdot 3H_2O) + 3CO_2 \longrightarrow (3CaCO_3 \cdot 2SiO_2 \cdot 3H_2O), \tag{2.5}$$

$$(2CaO \cdot SiO_2) + 2CO_2 + \nu H_2O \longrightarrow (SiO_2 \cdot \nu H_2O) + 2CaCO_3, \tag{2.6}$$

$$(3CaO \cdot SiO_2) + 3CO_2 + \nu H_2O \longrightarrow (SiO_2 \cdot \nu H_2O) + 3CaCO_3, \tag{2.7}$$

respectively. The coefficient ν is an arbitrary positive number of moles of water that is conserved through the reactions (2.6) and (2.7). Note that these reactions, especially (2.6) and (2.7), take place in the matrix space and therefore, the water entering in these reactions is not assumed to be mobile. Moreover, also note that the carbonation reactions (2.6) and (2.7) do not directly affect

the alkalinity of the concrete. We may account for this scenario provided the concrete is sufficiently wet and all phases are available to CO_2.

In general, CSH has a variable stoichiometry. There are at least five different morphologies of CSH-phases which grow during the hydration process [cf. SD96, CTTJ04, DdNC05, e.g.]. In this approach, the exact morphology is not relevant and for definiteness, we restrict ourselves to the stoichiometric combination (3-2-3) (also cf. section 5). Amorphous silica gel and calcium carbonate are usually the end products of cement phases carbonation (see [KK01], [Sis04, p. 22] and references therein).

2.3 Active concentrations

We define the active concentrations (in grams per cm^3) by:

$c_{CO_2(g)}$	–	concentration of CO_2 in pore air,
c_{CO_2}	–	concentration of CO_2 in pore water,
$c_{Ca(OH)_2}$	–	concentration of $Ca(OH)_2$,
w	–	concentration of (mobile) moisture,
c_{CaCO_3}	–	concentration of $CaCO_3$,
c_{CSH}	–	concentration of CSH,
c_{C_2S}	–	concentration of C_2S,
c_{C_3S}	–	concentration of C_3S.

We refer to w as *total humidity*, or *total moisture*, or simply, moisture – in all cases this variable encorporates the pore water and the vapors from the air-filled parts of the pore. However, it does not include the immobile water stored in the porous matrix (like gel water, e.g.).

3 Mass balances

Before formulating the mass balances of the active species, we introduce the specific form of the production terms.

3.1 Production terms

The kinetics of the carbonation and hydration reactions are assumed to be of power-law type [cf. FB90, e.g.]. While we assume *standard* reaction-rate constants for the carbonation reaction (2.5)–(2.7) and the hydration reactions (2.2), (2.3), an *improved* reaction constant is used for the rate constant of the carbonation reaction of $Ca(OH)_2$. It incorporates the fact that the rapidness of this reaction depends on the moisture potential w. We only give a short summary here. For more details see [MPMB05]. Other production terms due to dissolution, precipitation and exchange with the environment are discussed afterwards.

3.1.1 Production by hydration

The production terms by hydration, η_j^{hydr} for $j \in \{C_2S, C_3S\}$, are defined by means of power-law kinetics in the following way

$$\eta_j^{\text{hydr}} := C_j^{\text{hydr}} (c_j)^{p_j}, \tag{3.1}$$

where $C_j^{\text{hydr}} := k_j^{\text{hydr}} / (c_j^0)^{p_j - 1}$. Here, c_j^0 is the initial concentration of species j, while the factor k_j^{hydr} is the reaction constant for the (hydration) reaction between constituent j and water. The exponents p_j are the partial reaction orders of species j with respect to the hydration reaction. Following [PVF89], we choose $p_{C_2S} = 3.10$, $p_{C_3S} = 2.65$. Therefore, we define the production terms

due to hydration by

$$f^{\text{hydr}}_{\text{C}_2\text{S}} := C^{\text{hydr}}_{\text{C}_2\text{S}}(c_{\text{C}_2\text{S}})^{p_{\text{C}_2\text{S}}} \quad \text{and} \quad f^{\text{hydr}}_{\text{C}_3\text{S}} := C^{\text{hydr}}_{\text{C}_3\text{S}}(c_{\text{C}_3\text{S}})^{p_{\text{C}_3\text{S}}}. \tag{3.2}$$

3.1.2 Production by carbonation

We define the reaction rate of reaction (2.4) as

$$\eta^{\text{reac}}_{\text{Ca(OH)}_2} := C^{\text{reac}}_{\text{Ca(OH)}_2} f^{\text{hum}}(w) c^p_{\text{CO}_2} c^q_{\text{Ca(OH)}_2}, \tag{3.3}$$

where $C^{\text{reac}}_{\text{Ca(OH)}_2}$ is the reaction constant. For the partial orders of reaction p, q, we assume $p, q \geq 1$. The factor $f^{\text{hum}}(w)$ is defined as

$$f^{\text{hum}}(w) := g^{\text{hum}}(\text{RH}(w)). \tag{3.4}$$

RH is the relative humidity calculated from w. The equilibrium with the *relative humidity* RH is implicitly assumed by using an *sorption isotherm* $\text{RH}(w)$. For a range of $\text{RH} \in [50\%, 80\%]$ the sorption isotherm can be well approximated by an affine function, namely

$$\text{RH}(w) = a + b \cdot \phi \cdot w, \tag{3.5}$$

where a and b are porosity-dependent fitting parameters from [Ste00], see table 1 in the appendix for their values. The *clipping factor* (3.4) describes the dependence of the carbonation kinetics on RH. According to [Ste00, SSV93], it can be written as

$$g^{\text{hum}}(\text{RH}) := \begin{cases} 0, & \text{RH} \leq 0.5, \\ 5/2(\text{RH} - 0.5), & 0.5 < \text{RH} \leq 0.9, \\ 1, & \text{RH} > 0.9. \end{cases} \tag{3.6}$$

We are only aware of few references where possible values for $C^{\text{reac}}_{\text{Ca(OH)}_2}$ are mentioned ([Ste00, IM01, Cha99], e.g., in case of a first-order kinetics w.r.t. CO_2).

To point out the structure of the carbonation-reaction rates of reactions (2.5)–(2.7), we follow the modelling ideas in [PVF89]. For $j \in \{\text{CSH}, \text{C}_2\text{S}, \text{C}_3\text{S}\}$, we define the production terms by carbonation by as

$$\eta^{\text{reac}}_j := C^{\text{reac}}_j c_{\text{CO}_2}, \tag{3.7}$$

where $C^{\text{reac}}_j := k^{\text{reac}}_j a^{\text{s}}_j$ and k^{reac}_j is the reaction constant for the reaction between the constituent j and $\text{CO}_2(aq)$. The factor a^{s}_j represents the liquid-exposed surface area of the constituent j. There is some uncertainty about the ratio of the constants of reactions (2.4) and (2.5). For this, only a lower estimate can be obtained from the literature, namely $\frac{k^{\text{reac}}_j}{k^{\text{reac}}_{\text{Ca(OH)}_2}} > 2.4 \cdot 10^{-3}$ [cf. PVF89]. For the simulations we select a value for k^{reac}_j such that the latter estimate is satisfied. Then, we point out the effect of varying k^{reac}_j on the penetration depth. Therefore, we define the local carbonation-reaction terms as

$$f^{\text{reac}}_{\text{Ca(OH)}_2} := C^{\text{reac}}_{\text{Ca(OH)}_2} f^{\text{hum}}(w) c^p_{\text{CO}_2} c^q_{\text{Ca(OH)}_2}, \tag{3.8a}$$

$$f^{\text{reac}}_{\text{CSH}} := C^{\text{reac}}_{\text{CSH}} \Theta(c_{\text{CSH}}) c_{\text{CO}_2}, \tag{3.8b}$$

$$f^{\text{reac}}_{\text{C}_2\text{S}} := C^{\text{reac}}_{\text{C}_2\text{S}} \Theta(c_{\text{C}_2\text{S}}) c_{\text{CO}_2}, \tag{3.8c}$$

$$f^{\text{reac}}_{\text{C}_3\text{S}} := C^{\text{reac}}_{\text{C}_3\text{S}} \Theta(c_{\text{C}_3\text{S}}) c_{\text{CO}_2}, \tag{3.8d}$$

where $\Theta \colon \mathbb{R} \to \{0, 1\}$ is the Heaviside function,

$$\Theta(u) = \begin{cases} 1, & u > 0, \\ 0, & u \leq 0. \end{cases} \tag{3.9}$$

3.1.3 Other production terms and boundary conditions

We model the interfacial mass transfer from pore air to pore water by means of Henry's law. The corresponding production term has the form

$$f^{\text{Henry}} := C^{\text{ex}} \left(C^{\text{Henry}} c_{\text{CO}_2(g)} - c_{\text{CO}_2} \right), \tag{3.10}$$

where C^{ex} is the interfacial mass-transfer coefficient and C^{Henry} is the dimensionless Henry constant.

We implicitly assume instantaneous dissolution and precipitation of some of the carbonation reactants and products. Moreover, we assume homogeneous Neumann boundary conditions for all diffusing species at the interior boundary. At the exterior boundary, Robin boundary conditions are assumed for $c_{\text{CO}_2(g)}$ and w while homogeneous Neumann boundary conditions are applied for all other diffusing species. The fluxes across the external boundary are expressed as

$$\eta^{\text{Rob}}_{\text{CO}_2(g)} := C^{\text{Rob}}_{\text{CO}_2(g)}(c_{\text{CO}_2(g)} - c^{\text{ext}}_{\text{CO}_2(g)}), \tag{3.11a}$$

$$\eta^{\text{Rob}}_{\text{H}_2\text{O}} := C^{\text{Rob}}_{\text{H}_2\text{O}}(w - w^{\text{ext}}), \tag{3.11b}$$

where the constants C^{Rob}_j represent mass-transfer coefficients at the external boundary and $c^{\text{ext}}_{\text{CO}_2(g)}$ and w^{ext} are given exterior concentration of CO_2 and the moisture potential, respectively.

3.2 Mass balances of active species

We formulate the macroscopic mass balances for CO_2 in both phases (gaseous and liquid) and for $Ca(OH)_2$, $CaCO_3$, CSH, C_2S and C_3S in the liquid phase. The fact that the latter species should actually be associated with the solid matrix is taken care of via the structure of the reaction-rate constants. For moisture, we assume a local equilibrium of the gas and liquid phase [see Ste00, Arf98, Gru97, e.g.]. Moreover, we do not further distinguish between the products $3CaCO_3 \cdot 2SiO_2 \cdot 3H_2O$ and $3CaCO_3$. A more detailed description on the general modelling aspects of the carbonation problem can be found in [BKM03b, BKM03a, Mun05].

We formulate the system of reaction-diffusion equations independent of the space dimension. The time interval of interest is denoted by S. For numerical simulations, we only consider the case of one space dimension. In the formulation of the mass balances, we make use of some additional notation, namely m_j (the molar mass of species j) and D_j (the microscopic diffusivity of species j), ν (the outer normal unit vector), and the superscript 0 which denotes initial concentrations. Based on the discussion in the previous subsections, the complete model can be formulated in the following manner:

Mass balance for $CO_2(g)$:

$$\partial_t\big(\phi\phi^{\text{a}} c_{\text{CO}_2(g)}(x,t)\big) - \nabla \cdot \big(D_{\text{CO}_2(g)}\phi\phi^{\text{a}} \nabla c_{\text{CO}_2(g)}(x,t)\big) = -f^{\text{Henry}}(x,t), \quad x \in \Omega,\, t \in S, \tag{3.12a}$$

$$-(D_{\text{CO}_2(g)}\phi\phi^{\text{a}} \nabla c_{\text{CO}_2(g)}(x,t)) \cdot \nu = 0, \quad x \in \Gamma^{\text{N}},\, t \in S, \tag{3.12b}$$

$$-(D_{\text{CO}_2(g)}\phi\phi^{\text{a}} \nabla c_{\text{CO}_2(g)}(x,t)) \cdot \nu = C^{\text{Rob}}_{\text{CO}_2(g)}(c_{\text{CO}_2(g)}(x,t) - c^{\text{ext}}_{\text{CO}_2(g)}(x,t)), \quad x \in \Gamma^{\text{R}},\, t \in S, \tag{3.12c}$$

$$c_{\text{CO}_2(g)}(x,0) = c^0_{\text{CO}_2(g)}(x), \quad x \in \Omega. \tag{3.12d}$$

Mass balance for CO_2:

$$\partial_t\big(\phi\phi^{\text{w}} c_{\text{CO}_2}(x,t)\big) - \nabla \cdot \big(D_{\text{CO}_2}\phi\phi^{\text{w}} \nabla c_{\text{CO}_2}(x,t)\big) = f^{\text{Henry}}(x,t) \tag{3.13a}$$

$$+ m_{\text{CO}_2}\phi\phi^{\text{w}} \left(-f^{\text{reac}}_{\text{Ca(OH)}_2}(x,t) - 3f^{\text{reac}}_{\text{CSH}}(x,t) - 2f^{\text{reac}}_{\text{C}_2\text{S}}(x,t) - 3f^{\text{reac}}_{\text{C}_2\text{S}}(x,t) \right), \quad x \in \Omega,\, t \in S,$$

$$-(D_{\text{CO}_2}\phi\phi^{\text{w}} \nabla c_{\text{CO}_2}(x,t)) \cdot \nu = 0, \quad x \in \Gamma,\, t \in S, \tag{3.13b}$$

$$c_{\text{CO}_2}(x,0) = c^0_{\text{CO}_2}(x), \quad x \in \Omega. \tag{3.13c}$$

Mass balance for $Ca(OH)_2$:

$$\partial_t\big(\phi\phi^{\mathrm{w}} c_{\mathrm{Ca(OH)_2}}(x,t)\big) - \nabla\cdot\big(D_{\mathrm{Ca(OH)_2}}\phi\phi^{\mathrm{w}}\nabla c_{\mathrm{Ca(OH)_2}}(x,t)\big) \tag{3.14a}$$
$$= m_{\mathrm{Ca(OH)_2}}\phi\phi^{\mathrm{w}}\left(-f^{\mathrm{reac}}_{\mathrm{Ca(OH)_2}}(x,t) + \frac{1}{2}f^{\mathrm{hydr}}_{\mathrm{C_2S}}(x,t) + \frac{3}{2}f^{\mathrm{hydr}}_{\mathrm{C_3S}}(x,t)\right), \quad x\in\Omega,\, t\in S,$$
$$-(D_{\mathrm{Ca(OH)_2}}\phi\phi^{\mathrm{w}}\nabla c_{\mathrm{Ca(OH)_2}}(x,t))\cdot\nu = 0, \quad x\in\Gamma,\, t\in S, \tag{3.14b}$$
$$c_{\mathrm{Ca(OH)_2}}(x,0) = c^0_{\mathrm{Ca(OH)_2}}(x),\ x\in\Omega. \tag{3.14c}$$

Mass balance for (mobile) moisture:

$$\partial_t\big(\phi w(x,t)\big) - \nabla\cdot\big(D_{\mathrm{H_2O}}\phi\nabla w(x,t)\big) = m_{\mathrm{H_2O}}\phi\phi^{\mathrm{w}} f^{\mathrm{reac}}_{\mathrm{Ca(OH)_2}}(x,t), \quad x\in\Omega,\, t\in S, \tag{3.15a}$$
$$-(D_{\mathrm{H_2O}}\phi\nabla w(x,t))\cdot\nu = 0, \quad x\in\Gamma^{\mathrm{N}},\, t\in S, \tag{3.15b}$$
$$-(D_{\mathrm{H_2O}}\phi\nabla w(x,t))\cdot\nu = C^{\mathrm{Rob}}_{\mathrm{H_2O}}(w(x,t) - w^{\mathrm{ext}}(x,t)), \quad x\in\Gamma^{\mathrm{R}},\, t\in S, \tag{3.15c}$$
$$w(x,0) = w^0(x), \quad x\in\Omega. \tag{3.15d}$$

Mass balance for $CaCO_3$:

$$\partial_t\big(\phi\phi^{\mathrm{w}} c^{\mathrm{w}}_{\mathrm{CaCO_3}}(x,t)\big) \tag{3.16a}$$
$$= m_{\mathrm{CaCO_3}}\phi\phi^{\mathrm{w}}\left(f^{\mathrm{reac}}_{\mathrm{Ca(OH)_2}}(x,t) + 3f^{\mathrm{reac}}_{\mathrm{CSH}}(x,t) + 2f^{\mathrm{reac}}_{\mathrm{C_2S}}(x,t) + 3f^{\mathrm{reac}}_{\mathrm{C_3S}}(x,t)\right), \quad x\in\Omega,\, t\in S,$$
$$c_{\mathrm{CaCO_3}}(x,0) = c^0_{\mathrm{CaCO_3}}(x), \quad x\in\Omega. \tag{3.16b}$$

Mass balance for CSH:

$$\partial_t\big(\phi\phi^{\mathrm{w}} c^{\mathrm{w}}_{\mathrm{CSH}}(x,t)\big) \tag{3.17a}$$
$$= m_{\mathrm{CSH}}\phi\phi^{\mathrm{w}}\left(-f^{\mathrm{reac}}_{\mathrm{CSH}}(x,t) + \frac{1}{2}f^{\mathrm{hydr}}_{\mathrm{C_2S}}(x,t) + \frac{1}{2}f^{\mathrm{hydr}}_{\mathrm{C_3S}}(x,t)\right), \quad x\in\Omega,\, t\in S,$$
$$c_{\mathrm{CSH}}(x,0) = c^0_{\mathrm{CSH}}(x), \quad x\in\Omega. \tag{3.17b}$$

Mass balance for C_2S:

$$\partial_t\big(\phi\phi^{\mathrm{w}} c^{\mathrm{w}}_{\mathrm{C_2S}}(x,t)\big) = m_{\mathrm{C_2S}}\phi\phi^{\mathrm{w}}\left(-f^{\mathrm{reac}}_{\mathrm{C_2S}}(x,t) - f^{\mathrm{hydr}}_{\mathrm{C_2S}}(x,t)\right), \quad x\in\Omega,\, t\in S, \tag{3.18a}$$
$$c_{\mathrm{C_2S}}(x,0) = c^0_{\mathrm{C_2S}}(x), \quad x\in\Omega. \tag{3.18b}$$

Mass balance for C_3S:

$$\partial_t\big(\phi\phi^{\mathrm{w}} c^{\mathrm{w}}_{\mathrm{C_3S}}(x,t)\big) = m_{\mathrm{C_3S}}\phi\phi^{\mathrm{w}}\left(-f^{\mathrm{reac}}_{\mathrm{C_3S}}(x,t) - f^{\mathrm{hydr}}_{\mathrm{C_3S}}(x,t)\right), \quad x\in\Omega,\, t\in S, \tag{3.19a}$$
$$c_{\mathrm{C_3S}}(x,0) = c^0_{\mathrm{C_3S}}(x), \quad x\in\Omega. \tag{3.19b}$$

For consistency, we also included the factors $\phi\phi^{\mathrm{w}}$ in (3.17)–(3.19). Therefore, the formulation (3.12)–(3.19) is also true for porosities dependent on space or time.

4 Numerical implementation

In this section, we first present a weak formulation of the model (3.12)–(3.19). Afterwards, we perform a nondimensionalisation of all quantities which results in the final system of equations to be implemented using the finite element method [analogously as in MPMB05].

4.1 Weak formulation

We reformulate the system (3.12)–(3.19) in terms of macroscopic quantities. More precisely, we perform a transformation of the quantities from the previous section into volume-averaged concentrations of the form

$$\tilde{c}_{\mathrm{CO_2}(g)} := \phi\phi^{\mathrm{a}} c_{\mathrm{CO_2}(g)}, \qquad \tilde{c}_{\mathrm{CO_2}} := \phi\phi^{\mathrm{w}} c_{\mathrm{CO_2}}, \qquad \tilde{w} := \phi w, \quad \text{etc.} \tag{4.1}$$

We exclusively use the macroscopic quantities in the following, so – for ease of notation – we omit the tilde from now on. The main advantage of this procedure is that the porosities solely appear on the right-hand sides of the equations, i.e. in the production terms.

Define the spaces $\mathcal{V}$ and $\mathcal{W}$ as

$$\mathcal{V} = H^1(0,T;L^2(\Omega)), \tag{4.2}$$

$$\mathcal{W} = \{v \in L^2(0,T;H^1(\Omega)) \,|\, \partial_t v \in L^2(0,T;(H^1(\Omega))')\}, \tag{4.3}$$

and denote the $L^2(\Omega)$-scalar product by $(\,\cdot\,|\,\cdot\,)_\Omega$. Note that we have $\partial\Omega = \Gamma^{\mathrm{N}} \cup \Gamma^{\mathrm{R}}$ (disjoint). See [DL92] for the definition of the function spaces in (4.2) and (4.3).

The weak formulation of problem (3.12)–(3.19) in terms of macroscopic concentrations is given by

$$\begin{aligned} &c_{\mathrm{CO_2}(g)} \in \mathcal{W}, \quad c_{\mathrm{CO_2}(g)}(0) = \phi\phi^{\mathrm{a}} c^0_{\mathrm{CO_2}(g)} \quad \text{such that} \\ &(\partial_t c_{\mathrm{CO_2}(g)} \,|\, v)_\Omega + D_{\mathrm{CO_2}(g)}(\nabla c_{\mathrm{CO_2}(g)} \,|\, \nabla v)_\Omega \\ &\qquad = -(f^{\mathrm{Henry}} \,|\, v)_\Omega - C^{\mathrm{Rob}}_{\mathrm{CO_2}(g)}(c_{\mathrm{CO_2}(g)} - \phi\phi^{\mathrm{a}} c^{\mathrm{ext}}_{\mathrm{CO_2}(g)} \,|\, v)_{\Gamma^{\mathrm{R}}}, \end{aligned} \tag{4.4}$$

$$\begin{aligned} &c_{\mathrm{CO_2}} \in \mathcal{W}, \quad c_{\mathrm{CO_2}}(0) = \phi\phi^{\mathrm{w}} c^0_{\mathrm{CO_2}} \quad \text{such that} \\ &(\partial_t c_{\mathrm{CO_2}} \,|\, v)_\Omega + D_{\mathrm{CO_2}}(\nabla c_{\mathrm{CO_2}} \,|\, \nabla v)_\Omega = (f^{\mathrm{Henry}} \,|\, v)_\Omega \\ &\qquad + m_{\mathrm{CO_2}}(-f^{\mathrm{reac}}_{\mathrm{Ca(OH)_2}} - 3f^{\mathrm{reac}}_{\mathrm{CSH}} - 2f^{\mathrm{reac}}_{\mathrm{C_2S}} - 3f^{\mathrm{reac}}_{\mathrm{C_2S}}) \,|\, v)_\Omega, \end{aligned} \tag{4.5}$$

$$\begin{aligned} &c_{\mathrm{Ca(OH)_2}} \in \mathcal{W}, \quad c_{\mathrm{Ca(OH)_2}}(0) = \phi\phi^{\mathrm{w}} c^0_{\mathrm{Ca(OH)_2}} \quad \text{such that} \\ &(\partial_t c_{\mathrm{Ca(OH)_2}} \,|\, v)_\Omega + D_{\mathrm{Ca(OH)_2}}(\nabla c_{\mathrm{Ca(OH)_2}} \,|\, \nabla v)_\Omega = \\ &\qquad m_{\mathrm{Ca(OH)_2}}(-f^{\mathrm{reac}}_{\mathrm{Ca(OH)_2}} + \frac{1}{2} f^{\mathrm{hydr}}_{\mathrm{C_2S}}(x,t) + \frac{3}{2} f^{\mathrm{hydr}}_{\mathrm{C_3S}} \,|\, v)_\Omega \end{aligned} \tag{4.6}$$

$$\begin{aligned} &w \in \mathcal{W}, \quad w(0) = \phi w^0 \quad \text{such that} \\ &(\partial_t w \,|\, v)_\Omega + D_{\mathrm{H_2O}}(\nabla w \,|\, \nabla v)_\Omega = m_{\mathrm{H_2O}}(f^{\mathrm{reac}}_{\mathrm{Ca(OH)_2}} \,|\, v)_\Omega - C^{\mathrm{Rob}}_{\mathrm{H_2O}}(w - \phi w^{\mathrm{ext}} \,|\, v)_{\Gamma^{\mathrm{R}}}, \end{aligned} \tag{4.7}$$

where each equation needs to be satisfied for a.e. in S and all $v \in \mathcal{W}$ as well as

$$\begin{aligned} &c_{\mathrm{CaCO_3}} \in \mathcal{V}, \quad c_{\mathrm{CaCO_3}}(0) = \phi\phi^{\mathrm{w}} c^0_{\mathrm{CaCO_3}} \quad \text{such that} \\ &(\partial_t c_{\mathrm{CaCO_3}} \,|\, v)_\Omega = m_{\mathrm{CaCO_3}}(f^{\mathrm{reac}}_{\mathrm{Ca(OH)_2}} + 3f^{\mathrm{reac}}_{\mathrm{CSH}} + 2f^{\mathrm{reac}}_{\mathrm{C_2S}} + 3f^{\mathrm{reac}}_{\mathrm{C_3S}} \,|\, v)_\Omega, \end{aligned} \tag{4.8}$$

$$c_{\mathrm{CSH}} \in \mathcal{V},\ c_{\mathrm{CSH}}(0) = \phi\phi^{\mathrm{w}} c^0_{\mathrm{CSH}} \text{ such that } (\partial_t c_{\mathrm{CSH}} \,|\, v)_\Omega = m_{\mathrm{CSH}}(-f^{\mathrm{reac}}_{\mathrm{CSH}} + \frac{1}{2} f^{\mathrm{hydr}}_{\mathrm{C_2S}} + \frac{1}{2} f^{\mathrm{hydr}}_{\mathrm{C_3S}} \,|\, v)_\Omega, \tag{4.9}$$

$$c_{\mathrm{C_2S}} \in \mathcal{V},\ c_{\mathrm{C_2S}}(0) = \phi\phi^{\mathrm{w}} c^0_{\mathrm{C_2S}} \text{ such that } (\partial_t c_{\mathrm{C_2S}} \,|\, v)_\Omega = m_{\mathrm{C_2S}}(-f^{\mathrm{reac}}_{\mathrm{C_2S}} - f^{\mathrm{hydr}}_{\mathrm{C_2S}} \,|\, v)_\Omega, \tag{4.10}$$

$$c_{\mathrm{C_3S}} \in \mathcal{V},\ c_{\mathrm{C_3S}}(0) = \phi\phi^{\mathrm{w}} c^0_{\mathrm{C_3S}} \text{ such that } (\partial_t c_{\mathrm{C_3S}} \,|\, v)_\Omega = m_{\mathrm{C_3S}}(-f^{\mathrm{reac}}_{\mathrm{C_3S}} - f^{\mathrm{hydr}}_{\mathrm{C_3S}} \,|\, v)_\Omega, \tag{4.11}$$

where each equation needs to be satisfied a.e. in S for all $v \in \mathcal{V}$. Some of the production terms

need to be re-defined due to the switch from microscopic to macroscopic quantities. These are

$$f^{\text{Henry}} := C^{\text{ex}}(C^{\text{Henry}}(\phi\phi^{\text{a}})^{-1}c_{\text{CO}_2(g)} - (\phi\phi^{\text{w}})^{-1}c_{\text{CO}_2}), \tag{4.12}$$

$$f^{\text{reac}}_{\text{Ca(OH)}_2} := C^{\text{reac}}_{\text{Ca(OH)}_2} f^{\text{hum}}(\phi^{-1}w)(\phi\phi^{\text{w}})^{1-p-q}(c_{\text{CO}_2})^p(c_{\text{Ca(OH)}_2})^q, \tag{4.13}$$

$$f^{\text{hydr}}_{\text{C}_2\text{S}} := C^{\text{hydr}}_{\text{C}_2\text{S}}(\phi\phi^{\text{w}})^{1-p_{\text{C}_2\text{S}}}(c_{\text{C}_2\text{S}})^{p_{\text{C}_2\text{S}}}, \tag{4.14}$$

$$f^{\text{hydr}}_{\text{C}_3\text{S}} := C^{\text{hydr}}_{\text{C}_3\text{S}}(\phi\phi^{\text{w}})^{1-p_{\text{C}_3\text{S}}}(c_{\text{C}_3\text{S}})^{p_{\text{C}_3\text{S}}}. \tag{4.15}$$

4.2 Nondimensionalisation

We introduce the following nondimensional quantities,

$$\begin{aligned} &u_1 := c_{\text{CO}_2(g))}/c^{\text{m}}_1, && u_2 := c_{\text{CO}_2}/c^{\text{m}}_2, && u_3 := c_{\text{Ca(OH)}_2}/c^{\text{m}}_3, \\ &u_4 := w/c^{\text{m}}_4, && u_5 := c_{\text{CaCO}_3}/c^{\text{m}}_5, && u_6 := c_{\text{CSH}}/c^{\text{m}}_6, \\ &u_7 := c_{\text{C}_2\text{S}}/c^{\text{m}}_7, && u_8 := c_{\text{C}_3\text{S}}/c^{\text{m}}_8, \end{aligned} \tag{4.16}$$

where c^{m}_j, $j = 1, \ldots, 8$, are some *maximal concentrations*. In order to make a reasonable choice for the c^{m}_j and to simplify the model, we make the following *assumptions*:

1. $c_{\text{CO}_2(g)}(0) = c_{\text{CO}_2}(0) = c_{\text{CaCO}_3}(0) = 0$.
2. $c^{\text{ext}}_{\text{CO}_2(g)}$, w^{ext}, $c^0_{\text{Ca(OH)}_2}$, w^0, $c^0_{\text{CaCO}_3}$, c^0_{CSH}, $c^0_{\text{C}_2\text{S}}$, $c^0_{\text{C}_3\text{S}}$ are positive constants.
3. Diffusion of the species in water is sufficiently slow compared to diffusion in air.

Note that assumptions 1–3 are not inevitable but very much simplify making an appropriate choice for the c^{m}_j. They lead to the following definitions of the maximal concentrations:

$$\begin{aligned} c^{\text{m}}_1 &:= \phi\phi^{\text{a}}c^{\text{ext}}_{\text{CO}_2(g)}, \\ c^{\text{m}}_2 &:= \phi\phi^{\text{w}}C^{\text{Henry}}c^{\text{ext}}_{\text{CO}_2(g)}, \\ c^{\text{m}}_3 &:= \phi\phi^{\text{w}}c^0_{\text{Ca(OH)}_2} + \frac{1}{2}\frac{m_{\text{Ca(OH)}_2}}{m_{\text{C}_2\text{S}}}\phi\phi^{\text{w}}c^0_{\text{C}_2\text{S}} + \frac{3}{2}\frac{m_{\text{Ca(OH)}_2}}{m_{\text{C}_3\text{S}}}\phi\phi^{\text{w}}c^0_{\text{C}_3\text{S}}, \\ c^{\text{m}}_4 &:= \max\left\{\frac{m_{\text{H}_2\text{O}}}{m_{\text{Ca(OH)}_2}}c^{\text{m}}_3 + \phi w^0,\ \phi w^{\text{ext}}\right\}, \\ c^{\text{m}}_5 &:= \frac{m_{\text{CaCO}_3}}{m_{\text{Ca(OH)}_2}}c^{\text{m}}_3 + 3\frac{m_{\text{CaCO}_3}}{m_{\text{CSH}}}c^{\text{m}}_6 + 2\frac{m_{\text{CaCO}_3}}{m_{\text{C}_2\text{S}}}c^{\text{m}}_7 + 3\frac{m_{\text{CaCO}_3}}{m_{\text{C}_3\text{S}}}c^{\text{m}}_8, \\ c^{\text{m}}_6 &:= \phi\phi^{\text{w}}c^0_{\text{CSH}} + \frac{1}{2}\frac{m_{\text{CSH}}}{m_{\text{C}_2\text{S}}}\phi\phi^{\text{w}}c^0_{\text{C}_2\text{S}} + \frac{1}{2}\frac{m_{\text{CSH}}}{m_{\text{C}_3\text{S}}}\phi\phi^{\text{w}}c^0_{\text{C}_3\text{S}}, \\ c^{\text{m}}_7 &:= \phi\phi^{\text{w}}c^0_{\text{C}_2\text{S}}, \\ c^{\text{m}}_8 &:= \phi\phi^{\text{w}}c^0_{\text{C}_3\text{S}}. \end{aligned} \tag{4.17}$$

Define a *characterisitic diffusion time* for the fastest species involved, $\text{CO}_2(g)$, as

$$T := L^2/D_{\text{CO}_2(g)}, \tag{4.18}$$

and let $\tilde{t} := t/T$ and $\tilde{x} := x/L$ be the nondimensional time and space coordinates. An analogous nondimensionalisation was also used for the model considered in [MPMB05].

With definitions (4.16)–(4.18) we are led to the introduction of the following dimensionless combinations,

$$
\begin{aligned}
&\beta_2 := \frac{c_2^{\mathrm{m}}}{c_1^{\mathrm{m}}}, \qquad \beta_3 := \frac{c_3^{\mathrm{m}} m_{\mathrm{CO_2}}}{c_1^{\mathrm{m}} m_{\mathrm{Ca(OH)_2}}}, \qquad \beta_4 := \frac{c_4^{\mathrm{m}} m_{\mathrm{CO_2}}}{c_1^{\mathrm{m}} m_{\mathrm{H_2O}}}, \qquad \beta_5 := \frac{c_5^{\mathrm{m}} m_{\mathrm{CO_2}}}{c_1^{\mathrm{m}} m_{\mathrm{CaCO_3}}},\\
&\beta_6 := \frac{c_6^{\mathrm{m}} m_{\mathrm{CO_2}}}{c_1^{\mathrm{m}} m_{\mathrm{CSH}}}, \qquad \beta_7 := \frac{c_7^{\mathrm{m}} m_{\mathrm{CO_2}}}{c_1^{\mathrm{m}} m_{\mathrm{C_2S}}}, \qquad \beta_8 := \frac{c_8^{\mathrm{m}} m_{\mathrm{CO_2}}}{c_1^{\mathrm{m}} m_{\mathrm{C_3S}}},\\
&\delta_2 := \frac{D_{\mathrm{CO_2}}}{D_{\mathrm{CO_2}(g)}}, \qquad \delta_3 := \frac{D_{\mathrm{Ca(OH)_2}}}{D_{\mathrm{CO_2}(g)}}, \qquad \delta_4 := \frac{D_{\mathrm{H_2O}}}{D_{\mathrm{CO_2}(g)}},\\
&W^{\mathrm{Hen}} := \frac{L^2}{D_{\mathrm{CO_2}(g)}} C^{\mathrm{ex}}, \qquad W_1^{\mathrm{Rob}} := \frac{L}{D_{\mathrm{CO_2}(g)}} C^{\mathrm{Rob}}_{\mathrm{CO_2}(g)}, \qquad W_4^{\mathrm{Rob}} := \frac{L}{D_{\mathrm{CO_2}(g)}} C^{\mathrm{Rob}}_{\mathrm{H_2O}},\\
&\Phi^2 := \frac{L^2 m_{\mathrm{CO_2}} (c_2^{\mathrm{m}})^p (c_3^{\mathrm{m}})^q}{D_{\mathrm{CO_2}(g)} c_1^{\mathrm{m}}} C^{\mathrm{reac}}_{\mathrm{Ca(OH)_2}}, \qquad (\textit{Thiele modulus})\\
&R_6 := \frac{L^2 m_{\mathrm{CO_2}} c_2^{\mathrm{m}}}{D_{\mathrm{CO_2}(g)} c_1^{\mathrm{m}}} C^{\mathrm{reac}}_{\mathrm{CSH}}, \qquad R_7 := \frac{L^2 m_{\mathrm{CO_2}} c_2^{\mathrm{m}}}{D_{\mathrm{CO_2}(g)} c_1^{\mathrm{m}}} C^{\mathrm{reac}}_{\mathrm{C_2S}}, \qquad R_8 := \frac{L^2 m_{\mathrm{CO_2}} c_2^{\mathrm{m}}}{D_{\mathrm{CO_2}(g)} c_1^{\mathrm{m}}} C^{\mathrm{reac}}_{\mathrm{C_3S}},\\
&H_7 := \frac{L^2 m_{\mathrm{CO_2}} (c_7^{\mathrm{m}})^{p_{\mathrm{C_2S}}}}{D_{\mathrm{CO_2}(g)} c_1^{\mathrm{m}}} C^{\mathrm{hydr}}_{\mathrm{C_2S}}, \qquad H_8 := \frac{L^2 m_{\mathrm{CO_2}} (c_8^{\mathrm{m}})^{p_{\mathrm{C_3S}}}}{D_{\mathrm{CO_2}(g)} c_1^{\mathrm{m}}} C^{\mathrm{hydr}}_{\mathrm{C_3S}}.
\end{aligned}
\tag{4.19}
$$

The parameters β_j are usually called *capacity factors*, whereas the δ_j are ratios comparing each diffusivity with that of $\mathrm{CO_2}(g)$, see [PVF89, MPMB05]. The *Thiele modulus* Φ^2 as well as the factors R_j describe the rapidness of the carbonation reactions where as the H_j describe the rapidness of the hydration reactions. Furthermore, the factors W^{Hen}, W_1^{Rob} and W_4^{Rob} account for the rapidness of the different types of interfacial mass transfer.

For notational purposes we finally define

$$
\begin{aligned}
&u_1^{\mathrm{ext}} := \frac{\phi \phi^{\mathrm{a}} c^{\mathrm{ext}}_{\mathrm{CO_2}(g)}}{c_1^{\mathrm{m}}}, \qquad u_4^{\mathrm{ext}} := \frac{\phi w^{\mathrm{ext}}}{c_4^{\mathrm{m}}}, \qquad u_4^0 := \frac{\phi w^0}{c_4^{\mathrm{m}}}, \qquad u_5^0 := \frac{\phi \phi^{\mathrm{w}} c^0_{\mathrm{CaCO_3}}}{c_5^{\mathrm{m}}},\\
&u_6^0 := \frac{\phi \phi^{\mathrm{w}} c^0_{\mathrm{CSH}}}{c_6^{\mathrm{m}}}, \qquad u_7^0 := \frac{\phi \phi^{\mathrm{w}} c^0_{\mathrm{C_2S}}}{c_7^{\mathrm{m}}}, \qquad u_8^0 := \frac{\phi \phi^{\mathrm{w}} c^0_{\mathrm{C_3S}}}{c_8^{\mathrm{m}}}
\end{aligned}
\tag{4.20}
$$

Transformation of system (4.4)–(4.11) to the dimensionless quantities yields the system of equations to be solved numerically:

$$
\begin{gathered}
u_1 \in \mathcal{W}, \quad u_1(0) = 0 \text{ such that}\\
(\partial_t u_1 \,|\, v)_\Omega + (\nabla u_1 \,|\, \nabla v)_\Omega = -(f^{\mathrm{Henry}} \,|\, v)_\Omega - W_1^{\mathrm{Rob}} (u_1 - u_1^{\mathrm{ext}} \,|\, v)_{\Gamma^{\mathrm{R}}},
\end{gathered}
\tag{4.21}
$$

$$
\begin{gathered}
u_2 \in \mathcal{W}, \quad u_2(0) = 0 \text{ such that}\\
\beta_2 (\partial_t u_2 \,|\, v)_\Omega + \beta_2 \delta_2 (\nabla u_2 \,|\, \nabla v)_\Omega = +(f^{\mathrm{Henry}} \,|\, v)_\Omega + (-f_3^{\mathrm{reac}} - 3 f_6^{\mathrm{reac}} - 2 f_7^{\mathrm{reac}} - 3 f_8^{\mathrm{reac}} \,|\, v)_\Omega,
\end{gathered}
\tag{4.22}
$$

$$
\begin{gathered}
u_3 \in \mathcal{W}, \quad u_3(0) = 1 \text{ such that}\\
\beta_3 (\partial_t u_3 \,|\, v)_\Omega + \beta_3 \delta_3 (\nabla u_3 \,|\, \nabla v)_\Omega = (-f_3^{\mathrm{reac}} + \frac{1}{2} f_7^{\mathrm{hydr}} + \frac{3}{2} f_8^{\mathrm{hydr}} \,|\, v)_\Omega,
\end{gathered}
\tag{4.23}
$$

$$
\begin{gathered}
u_4 \in \mathcal{W}, \quad u_4(0) = u_4^0 \text{ such that}\\
\beta_4 (\partial_t u_4 \,|\, v)_\Omega + \beta_4 \delta_4 (\nabla u_4 \,|\, \nabla v)_\Omega = (f_3^{\mathrm{reac}} \,|\, v)_\Omega - W_4^{\mathrm{Rob}} \beta_4 (u_4 - u_4^{\mathrm{ext}} \,|\, v)_{\Gamma^{\mathrm{R}}},
\end{gathered}
\tag{4.24}
$$

where each equation has to be satisfied for a.e. $t \in S$ and for all $v \in \mathcal{W}$ as well as

$$u_5 \in \mathcal{V},\ u_5(0) = 0 \text{ such that } \beta_5(\partial_t u_5 \,|\, v)_\Omega = (f_3^{\text{reac}} + 3f_6^{\text{reac}} + 2f_7^{\text{reac}} + 3f_8^{\text{reac}} \,|\, v)_\Omega \tag{4.25}$$

$$u_6 \in \mathcal{V},\ u_6(0) = u_6^0 \text{ such that } \beta_6(\partial_t u_6 \,|\, v)_\Omega = (-f_6^{\text{reac}} + \frac{1}{2}f_7^{\text{hydr}} + \frac{1}{2}f_8^{\text{hydr}} \,|\, v)_\Omega \tag{4.26}$$

$$u_7 \in \mathcal{V},\ u_7(0) = u_7^0 \text{ such that } \beta_7(\partial_t u_7 \,|\, v)_\Omega = (-f_7^{\text{reac}} - f_7^{\text{hydr}} \,|\, v)_\Omega \tag{4.27}$$

$$u_8 \in \mathcal{V},\ u_8(0) = u_8^0 \text{ such that } \beta_8(\partial_t u_8 \,|\, v)_\Omega = (-f_7^{\text{reac}} - f_8^{\text{hydr}} \,|\, v)_\Omega \tag{4.28}$$

where each equation has to be satisfied for a.e. $t \in S$ and for all $v \in \mathcal{V}$. The dimensionless production terms are

$$f^{\text{Henry}} := W^{\text{Hen}}(C^{\text{Hen}}(\phi\phi^{\text{a}})^{-1}u_1 - (\phi\phi_w)^{-1}\beta_2 u_2), \tag{4.29}$$

$$f_3^{\text{reac}} := \Phi^2(\phi\phi_w)^{1-p-q} f^{\text{hum}}(u_4 c_4^{\text{m}}\phi^{-1})u_2^p u_3^q, \tag{4.30}$$

$$f_j^{\text{reac}} := R_j\Theta(u_j)u_2, \quad j \in \{6,7,8\}, \tag{4.31}$$

$$f_k^{\text{hydr}} := H_k(\phi\phi_w)^{1-p_k}u_k^{p_k} \quad k \in \{7,8\}. \tag{4.32}$$

In the numerical implementation, we approximate the Heaviside function Θ by

$$\Theta^{\text{approx}}(x) := \frac{x}{x+\gamma} \tag{4.33}$$

for $x \geq 0$ with $0 < \gamma \ll 1$ in order to avoid numerical problems.

4.3 Carbonation depth

As discussed earlier, we are interested in the prediction of the carbonation penetration depth, i.e. in how far the carbonation reaction of $Ca(OH)_2$ has advanced into the concrete sample at any given time. We define the penetration depth to be the isoline which corresponds to a (dimensionless) $Ca(OH)_2$-concentration equal to 0.1,

$$s(t) := \{x \in \Omega \,|\, u_3(x,t) = 0.1\} \qquad \text{for each } t \in S. \tag{4.34}$$

Analogous definitions of the carbonation front can be found in [SSV95, SSV93], e.g. We follow here the way indicated in [Ste00, SDA02].

4.4 Numerical solution

The equations (4.21)–(4.28) form a weakly-coupled system of semi-linear parabolic partial and ordinary differential equations. As in [MPMB05], we solve it numerically in one space-dimension by using a standard finite element discretisation method. More precisely, we accomplish a semi-discretisation in space on a uniform mesh of width $h = 1/(n-1)$ by the Galerkin method. For the test and trial functions, first-order splines are used. In addition, we apply the standard mass-lumping-scheme, cf. [KA00], e.g. See [GM03] for a detailed description of a similar discretisation problem. The nonlinear terms f_j^{reac} and f_k^{hydr} are approximated by the trapezoidal rule.

The resulting stiff system of $8 \times n$ ODEs is numerically integrated using the MATLAB ODE stiff solver `ode15s`, which is a variable-order solver based on numerical-differentiation formulas (NDFs).[1]

The examples in the following section are obtained by choosing $n = 80$.

[1] See `www.mathworks.com` for details and further references.

5 Numerical simulation of an accelerated carbonation test

In figures 2 and 3, we show dimensionless concentration profiles of all involved species ($CO_2(g)$, $CO_2(aq)$, $Ca(OH)_2$, moisture, $CaCO_3$, CSH, C_2S and C_3S) as well as the carbonation depth. For this, we use a set of parameters for the accelerated carbonation scenario based on data from [PVF89] (cf. the appendix for values of the parameters). We refer to this set of parameters as the *standard set* in the sequel. The experimental data we are plotting for the carbonation depth is also due to [PVF89].

The characteristic time scale of the carbonation reaction of $Ca(OH)_2$ is essentially faster than the characteristic time scales of the carbonation reactions of the other species and of the hydration reactions. For the standard set of parameters, we have

$$\Phi^2 \approx 10^3, \quad R_6 \approx 7, \quad R_7 \approx 5, \quad R_8 \approx 4, \quad H_7 \approx 5 \cdot 10^{-4}, \quad H_8 \approx 2 \cdot 10^{-4}.$$

Moreover, the characteristic diffusion time scale of $CO_2(g)$ is considerably faster than those of all other species (we have $\delta_1 = 1$ while the second largest is $\delta_2 \approx 8 \cdot 10^{-6}$).

The present formulation does not allow the diffusion of the additional phases CSH, C_2S and C_3S. However, we also investigated what happens if they diffused with the diffusivity of ions in pore water. There is only a slight change in the quantitative results and none in the qualitative results. This is basically due to the fact that the ionic diffusivity is very small compared to that of $CO_2(g)$.

Compared to the simulation results of the simplified model [MPMB05], the concentration profiles shown in figures 2 and 3 differ only marginally, except that of $CaCO_3$ which now shows a bend in the decrease. This is due to the fact that in this model, there is more than one source producing $CaCO_3$. Moreover, the additional profiles of the concentrations of CSH, C_2S, and C_3S show a similar behaviour like that of $Ca(OH)_2$. It can be observed that due to hydration reactions, the concentrations of C_2S and C_3S also decrease in the uncarbonated part of the concrete sample while those of $CaCO_3$ and CSH increase. However, these effects are comparably small for the chosen set of parameters.

Note that assuming a constant moisture profile instead of choosing a PDE for moisture does not change the qualitative results. Even the quantitative change is fairly small since the moisture content only enters in the improved reaction rate of the carbonation reaction of $Ca(OH)_2$ (cf. 3.1). Moreover, we always choose the mass-transfer coefficients at the external boundary of the concrete sample very high in order to account for Dirichlet boundary conditions. This seems to be a standard choice when simulating accelerated carbonation tests. For a detailed discussion of the effect of the moisture on the carbonation penetration we refer to [MPMB05].

The CSH-phases admit several stoichiometries [cf. SD96]. In our model, we only account for a particular stoichiometry for CSH (namely, 3-2-3). This does not influence the qualitative results although other stoichiometries may consume more CO_2 when carbonating and they may also have different (carbonation-) reaction constants (they also have different molar masses). We investigate the effects due to a change of the carbonation-reaction constant in section 5.2.1. This numerical test may be thought of as considering different CSH stoichiometries.

Since an extensive study of the effects due to variations of some of the relevant parameters was performed for the simplified model in [MPMB05] (neglecting CSH, C_2S, and C_3S), we concentrate on additional effects basically due to the inclusion of the other phases. We investigate the influence of each carbonation reaction, in particular the consumption of CO_2 by each reaction and the alternate neglect of CSH, C_2S, and C_3S (cf. section 5.1) as well as the effects due to a variation of the carbonation- and hydration-rate constants (cf. section 5.2).

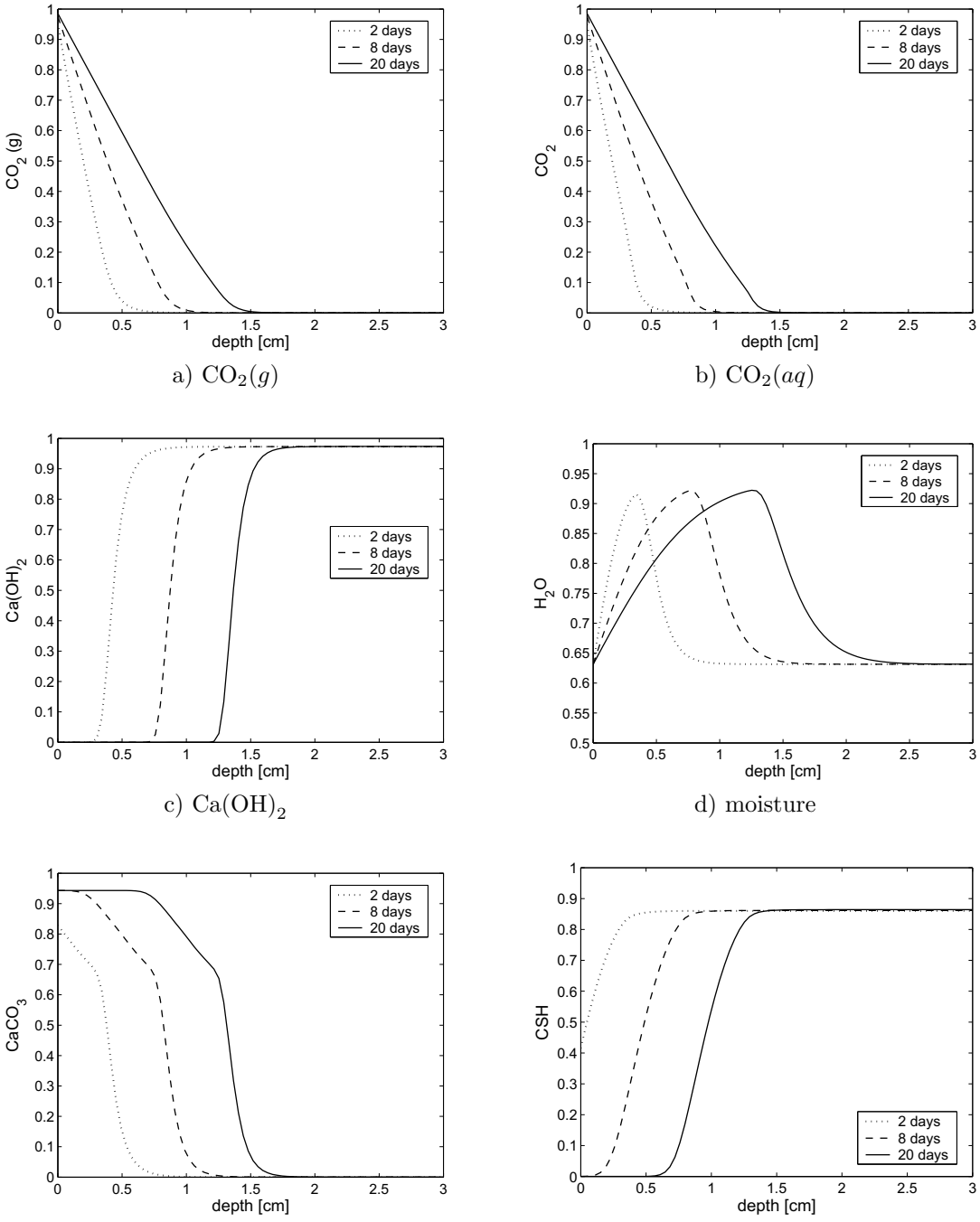

a) $CO_2(g)$ b) $CO_2(aq)$

c) $Ca(OH)_2$ d) moisture

e) $CaCO_3$ f) CSH

Figure 2: Concentration profiles of the involved species obtained with the standard set of parameters of the accelerated test.

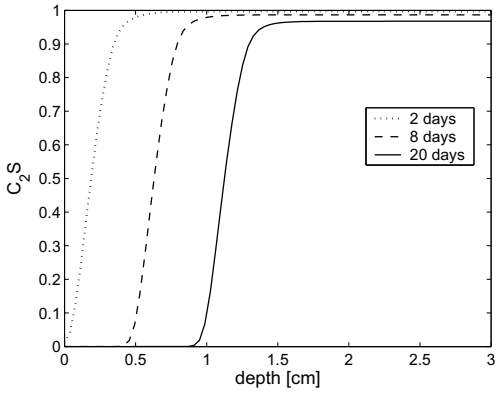

a) C_2S

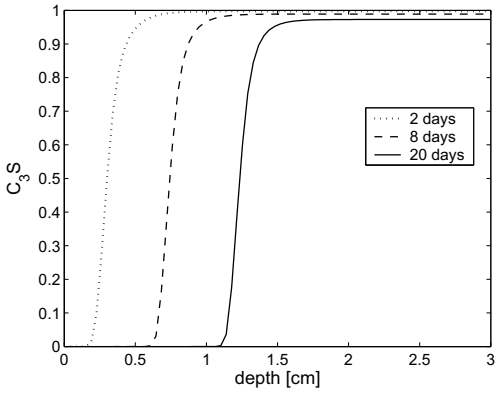

b) C_3S

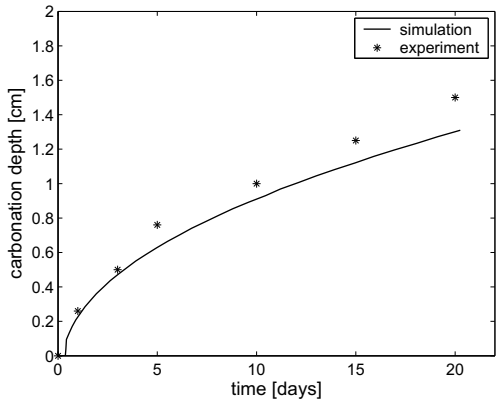

c) carbonation depth

Figure 3: Profiles of concentrations of C_2S and C_3S as well as carbonation depth obtained with the standard set of parameters of the accelerated test.

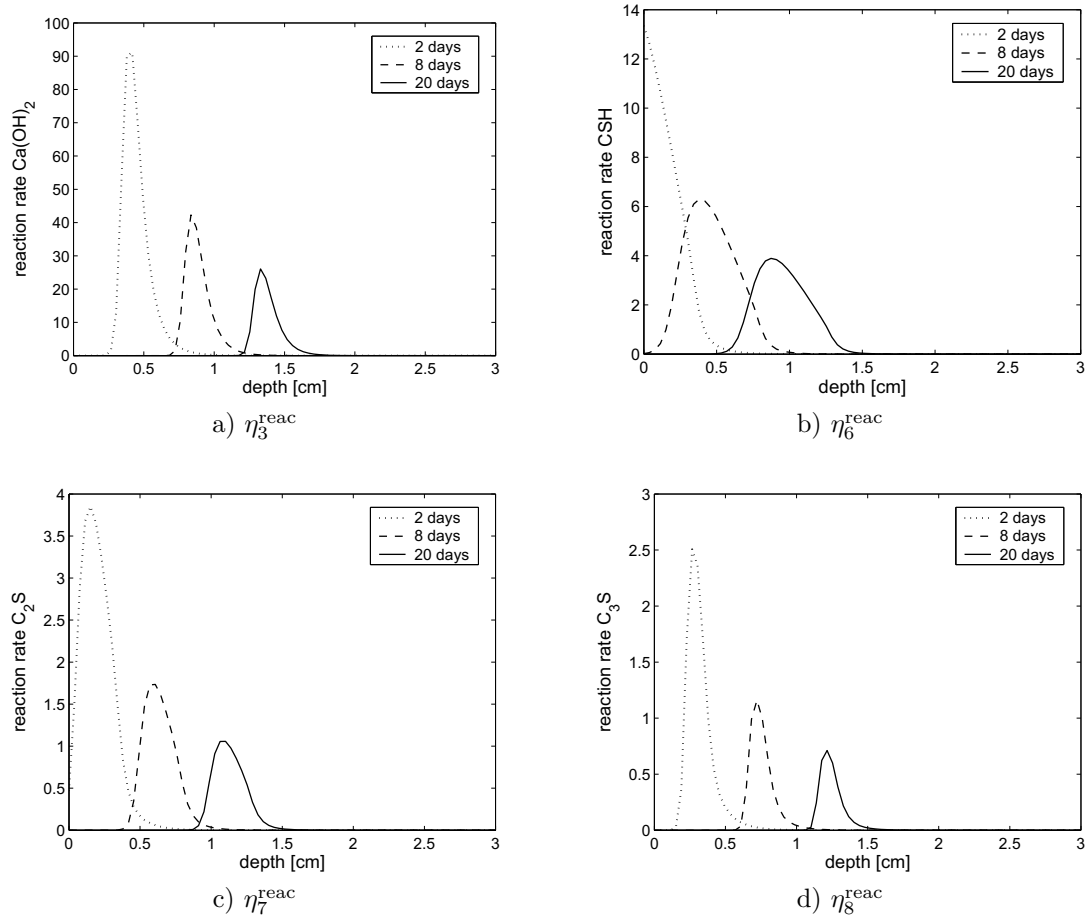

Figure 4: Dimensionless production terms of the different carbonation reactions.

5.1 Influence of the competition of parallel carbonation reactions

We want to compare the influence of each carbonation reaction on the penetration depth. In figure 4, the dimensionless production terms

$$\eta_j^{\mathrm{reac}} := n_j^{\mathrm{reac}} f_j^{\mathrm{reac}}, \quad j \in \{3, 6, 7, 8\}, \tag{5.1}$$

are plotted (with stoichiometric factors n_j^{reac} equal to 1, 3, 2 and 3 for j equal to 3, 6, 7 and 8, respectively).

It can be observed that the strongest carbonation reaction is that of $Ca(OH)_2$, followed by that of CSH. The reaction rates of C_2S and C_3S are essentially smaller. The reaction zone associated with $Ca(OH)_2$-depletion is the most narrow and most furthest advanced into the concrete sample at any given time. On the other hand, the reaction zone of CSH is the widest and also lagging behind the most. The reaction zone of C_2S is somewhere in between while that of C_3S is quite similar to that of $Ca(OH)_2$ (apart from the magnitude of the reaction rate). This last fact can be explained by the comparably small amount of C_3S available to carbonation.

Since we expect a strong competition for CO_2 by the three carbonation reactions, we are interested in how much CO_2 is consumed by each carbonation reaction. Moreover, since simpler models usually neglect CSH, C_2S, and C_3S, we are interested in how great their impact is on the carbonation of $Ca(OH)_2$. Therefore, we also consider two scenarios and compare them to the full scenario (cf. figs. 2 and 3): in the first, we neglect CSH, C_2S and C_3S; in the second, we neglect C_2S and C_3S.

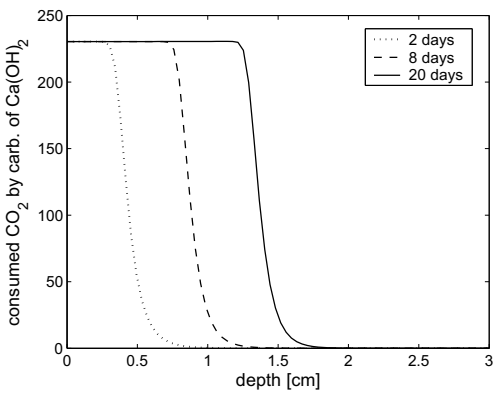

a) CO_2 consumed by carbonation of $Ca(OH)_2$

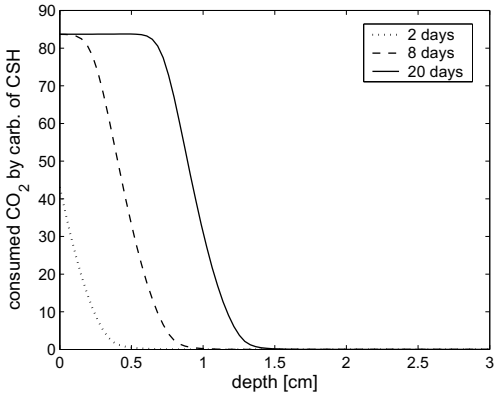

b) CO_2 consumed by carbonation of CSH

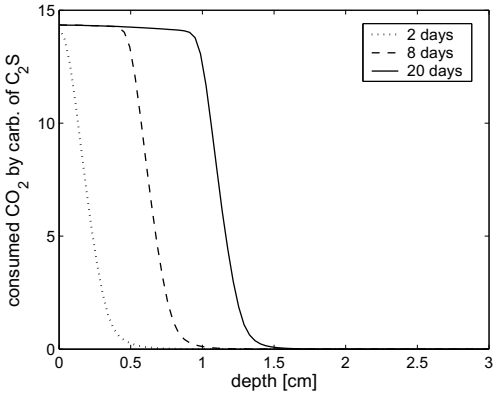

c) CO_2 consumed by carbonation of C_2S

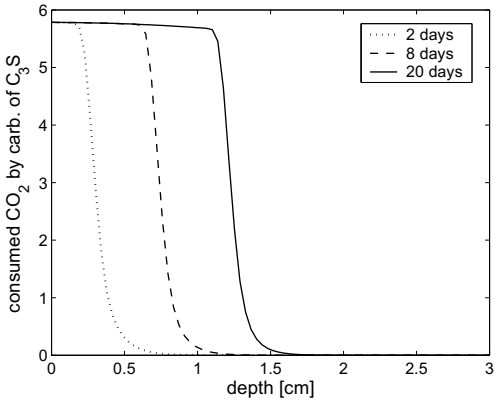

d) CO_2 consumed by carbonation of C_3S

Figure 5: Consumed CO_2 due to carbonation of the carbonatable species.

5.1.1 Consumption of CO_2 by each carbonation reaction

Since CSH, C_2S and C_3S cannot diffuse, we can calculate the amount of CO_2 which has been consumed due to each carbonation after any given time. We are particularly interested in the amount of CO_2 consumed by carbonation of each reactant. We denote this quantity with $P_j(x,t)$, $j \in \{3,6,7,8\}$. Note that this quantity satisfies the ordinary differential equation

$$\partial_t(\beta_2 P_j(x,t)) = n_j^{\text{reac}} f_j^{\text{reac}}, \quad x \in \Omega,\, t > 0, \qquad P_j(x,0) = 0. \tag{5.2}$$

The spatial profiles of $P_j(x,t)$ are plotted in figure 5.

It can be observed that all four species compete for CO_2. However, the amount of CO_2 consumed by the carbonation of $Ca(OH)_2$ is much greater than that of all other species. Namely, the amount consumed by carbonation of $Ca(OH)_2$ is four times as great as that of CSH, 16 times as great as that of C_2S and roughly 36 times as great as that of C_3S. It is also worth noting that the reaction zone associated with $Ca(OH)_2$ is always ahead of the other reaction zones. This agrees with the experimental observations in [Cha97].

5.1.2 Alternate neglect of CSH, C_2S, and C_3S

In this section we investigate the influence of each carbonation process on the penetration depth. Recall that the carbonation depth is defined via an a priori fixed isoline of the concentration profile

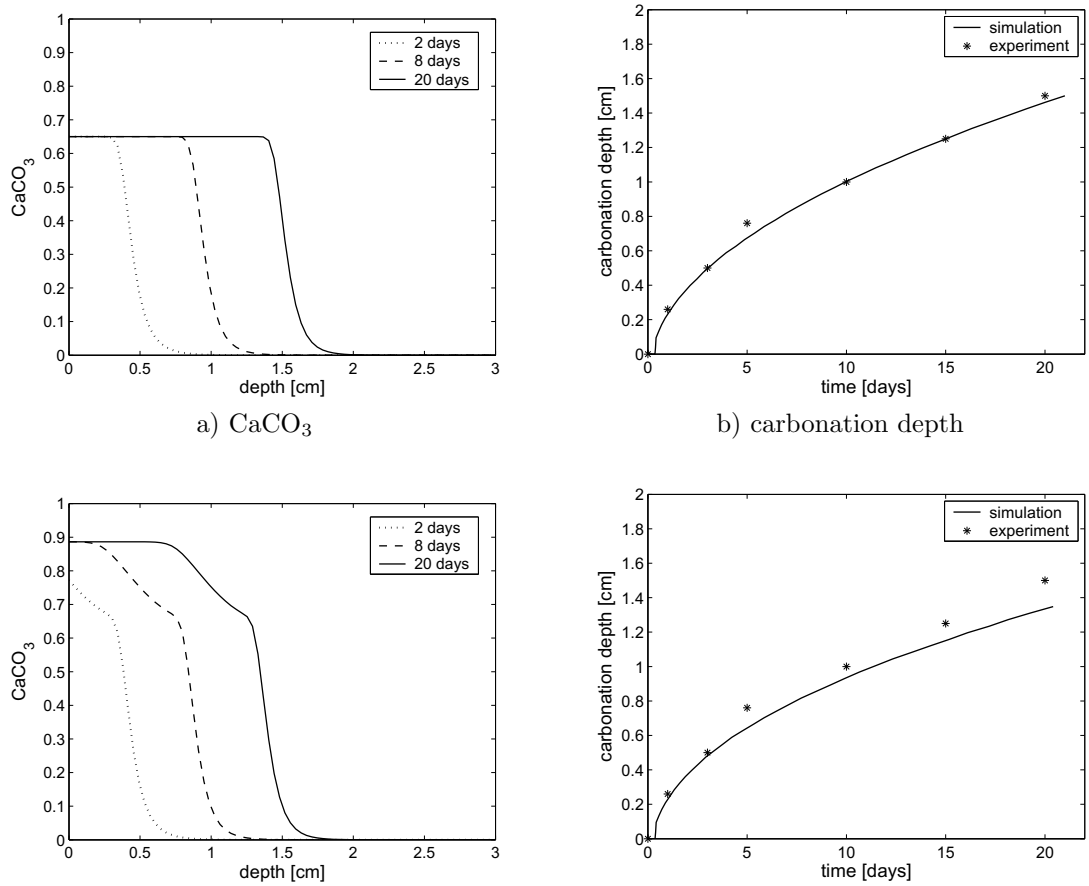

a) $CaCO_3$ b) carbonation depth

c) $CaCO_3$ d) carbonation depth

Figure 6: Profile of $CaCO_3$ and carbonation depth if CSH, C_2S and C_3S are neglected (a,b); and if C_2S and C_3S are neglected (c,d).

of $Ca(OH)_2$ (cf. sec. 4.3). Therefore, we consider the amount of produced $CaCO_3$ as well as the carbonation depth in two cases:

- neglect of CSH, C_2S, and C_3S,
- neglect of C_2S and C_3S.

These two scenarios are illustrated in figure 6 (also compare with the full scenario, figs. 2e and 3c). Note that since C_2S and C_3S do not consume much CO_2 compared to CSH and $Ca(OH)_2$, it is reasonable to consider them together.

It can be observed that the carbonation of CSH affects the simulated carbonation depth as it consumes CO_2 which would otherwise be available for carbonation of $Ca(OH)_2$. On the other hand, the influence of C_2S and C_3S is almost negligible.

5.2 Variation of carbonation- and hydration-rate constants

As the carbonation- and hydration-rate constants are somewhat uncertain [cf. PVF89, SD96, e.g.] we want to illustrate the effects due to their variation. The effect of the variation of the Thiele modulus on the carbonation penetration depth was extensively investigated in [MPMB05]. Therefore, we concentrate on the reaction and hydration rates of CSH, C_2S, and C_3S. Note that the influence of the additional species is already quite small which is why we only investigate the effect of faster rates.

5.2.1 Variation of carbonation-rate constants

In figure 7, the dimensionless production terms η_j^{reac} (also cf. (5.1)), the concentration profile of $CaCO_3$ as well as the carbonation depth are plotted for the standard setting, except that the reaction-rate constants of the carbonation of CSH, C_2S, and C_3S have been chosen ten times greater.

It can be observed that the carbonation depth is smaller than in the in the standard setting (figs. 2 and 3). This is due to the fact that more CO_2 is consumed by the carbonation of CSH, C_2S, and C_3S. Therefore, it is not available for carbonation of $Ca(OH)_2$. Moreover, the concentration profiles of CSH, C_2S and C_3S appear steeper and it can be seen that, in this setting, all reaction zones seem to coincide.

If the carbonation-rate constants of CSH, C_2S, and C_3S are chosen 100 times greater than in the standard setting it can be observed that the reaction zones of these additional phases overtake the one associated with $Ca(OH)_2$ (cf. fig. 8). It is not clear whether these observations reflect the reality. Nevertheless, it is due to the fact that there is not as much CSH, C_2S and C_3S available for carbonation as there is $Ca(OH)_2$. Therefore, these phases are used up more quickly and the reaction zone associated with them advances more quickly. As in the previous setting, the carbonation depth is only slightly affected, however. Regarding this last observation, recall again that the carbonation depth is defined via an isoline of the concentration profile of $Ca(OH)_2$ so that it does not recover this faster advancement of the reaction zones of the additional phases. It can also be observed that the maximum of the production term related to carbonation of $Ca(OH)_2$ increases (beside the maxima of the other production terms). This is due to the fact that, in this setting, the concentration of CO_2 at the position of the reaction zone is significantly higher (the profile of the CO_2-concentration changes only slightly compared to the standard setting).

If the reaction-rate constants of CSH, C_2S, and C_3S are chosen significantly smaller than in the standard setting (multiplying them by a factor of 1/10 or 1/100, e.g.) the influence of the additional phases just decreases steadily.

5.2.2 Variation of hydration-rate constants

In figure 9, selected concentration profiles as well as the carbonation depth are shown for the standard setting but with hydration-rate constants which have been chosen ten times faster than in figures 2 and 3.

Recall that the overall hydration process is assumed in its final phase. Therefore, it is almost complete at the beginning of our simulations. However, some small competition effects can be observed. The concentration profiles of C_2S and C_3S show a considerable deviation. The influence on the profiles of interest (the carbonation depth, e.g.) is rather small. Note that even a multiplication of the hydration-rate constants by a factor of 1000 does not have a significant effect on the carbonation depth.

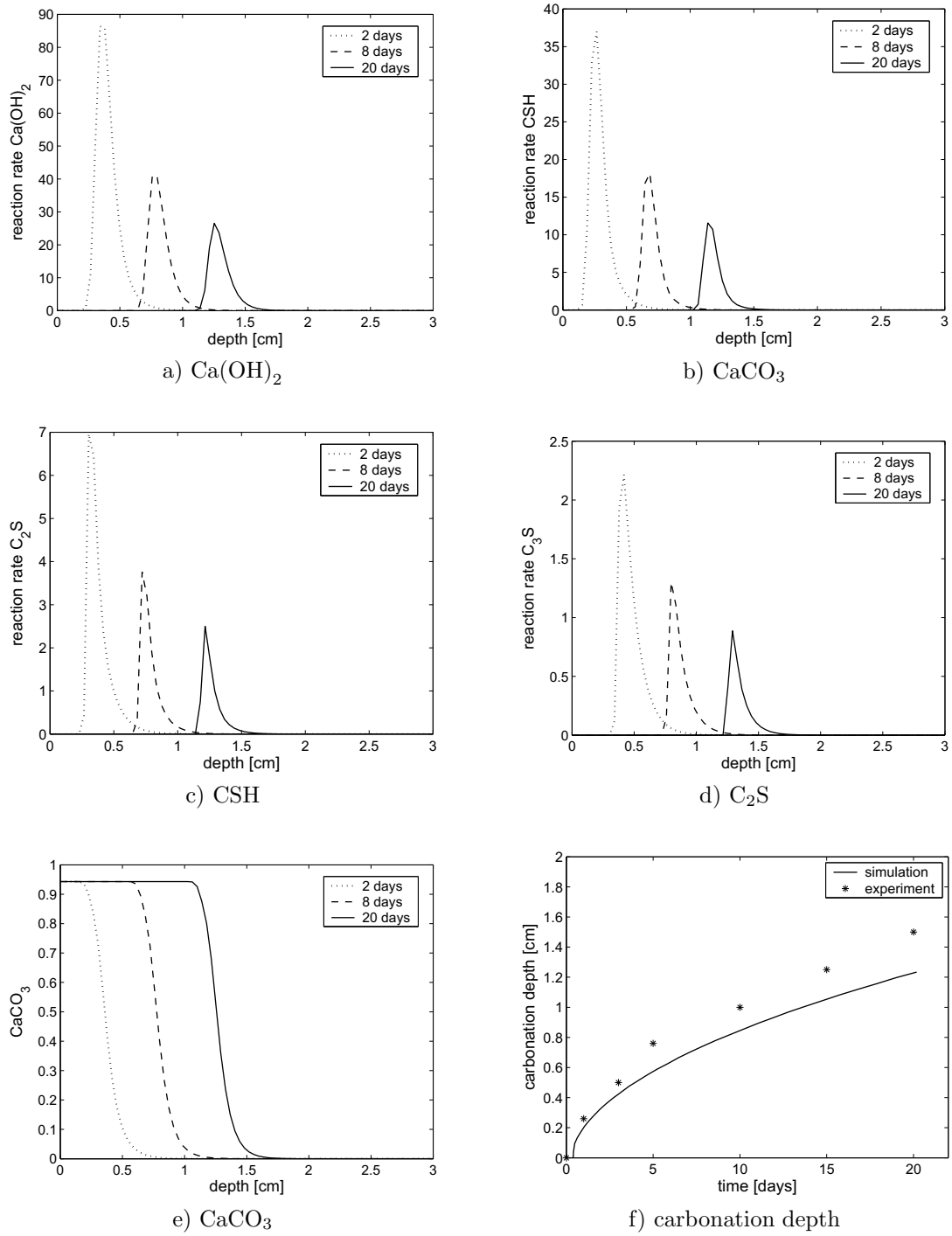

Figure 7: Production rates, profile of $CaCO_3$ as well as carbonation depth obtained with *carbonation-reaction rates* ten times faster than in the standard setting.

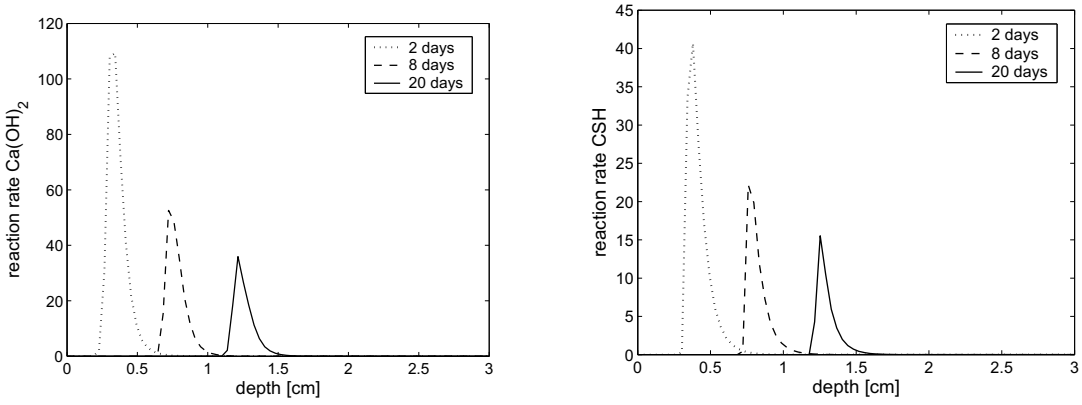

a) $Ca(OH)_2$

b) $CaCO_3$

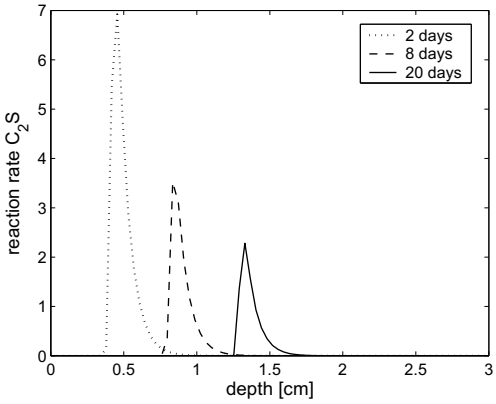

c) CSH

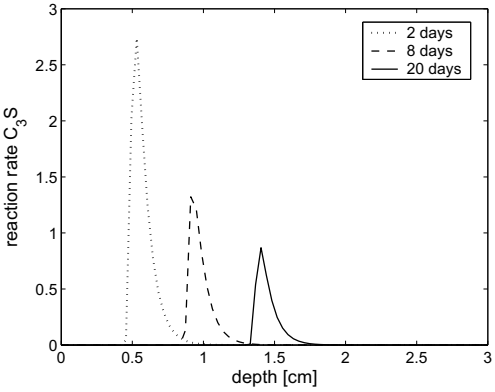

d) C_2S

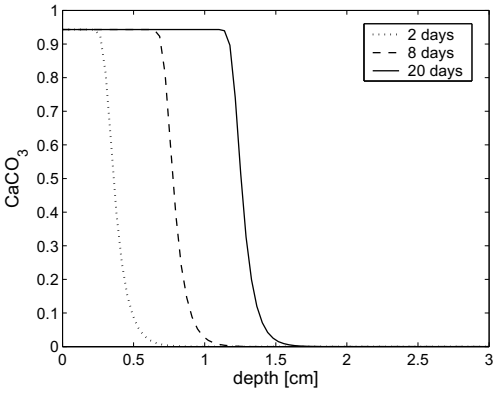

e) $CaCO_3$

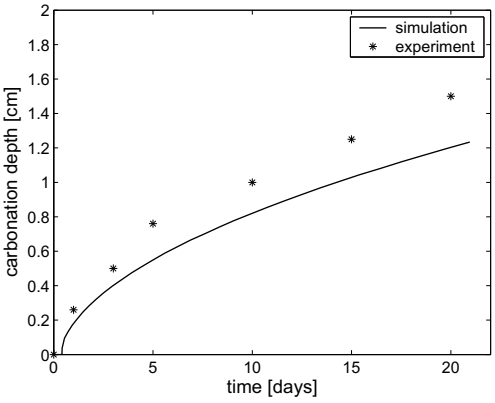

f) carbonation depth

Figure 8: Production rates, profile of $CaCO_3$ as well as carbonation depth obtained with *carbonation-reaction rates* one hundred times faster than in the standard setting.

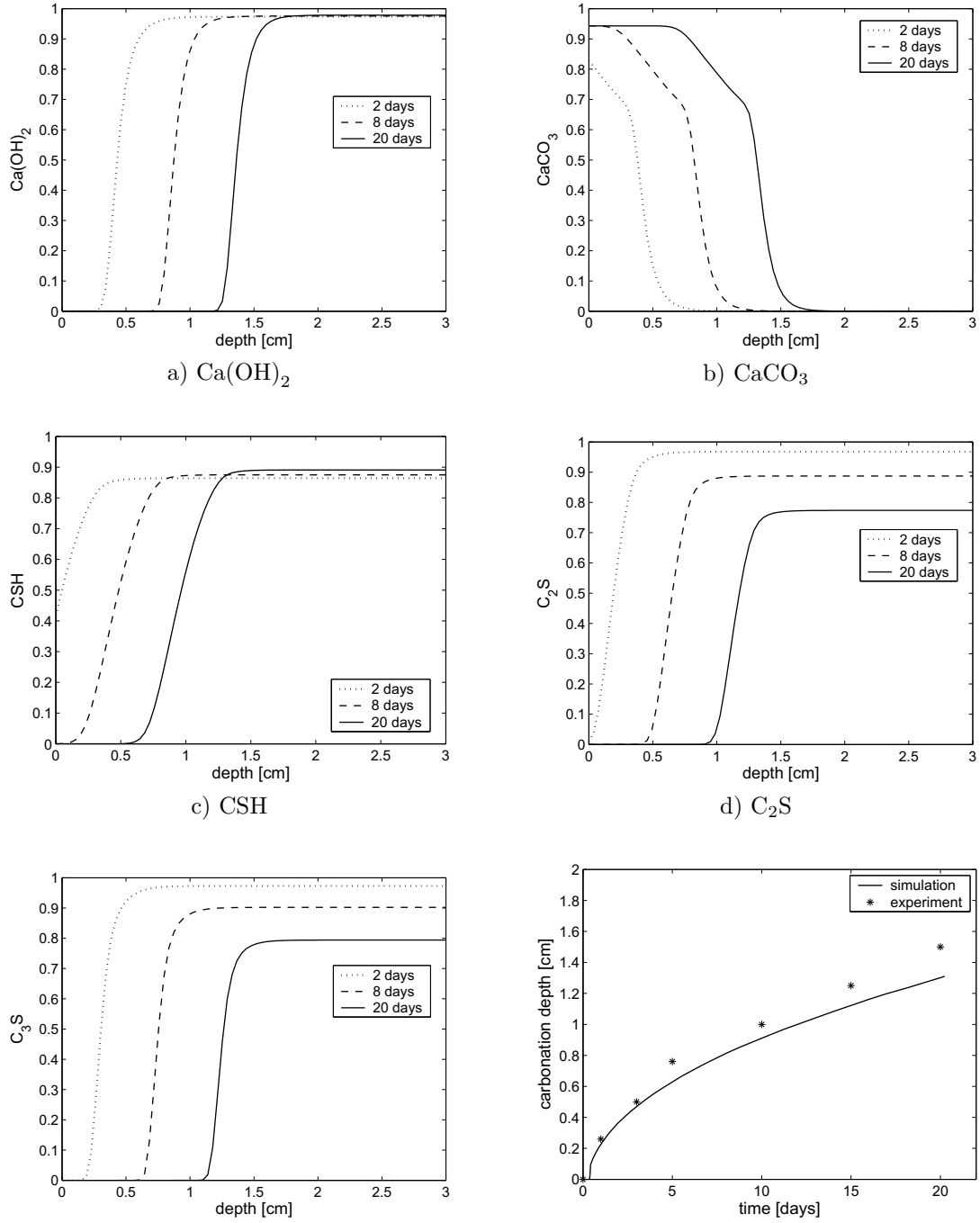

a) $Ca(OH)_2$ b) $CaCO_3$

c) CSH d) C_2S

e) C_3S f) carbonation depth

Figure 9: Profiles of selected concentrations as well as carbonation depth obtained with *hydration-reaction rates* ten times faster than in the standard setting.

6 Summary and discussion

The carbonation of concrete was investigated taking into account several parallel carbonation and hydration reactions. A closed system of reaction-diffusion equations was used to model the mass balances of all active species under consideration. To allow easy comparisons of the importance of the involved carbonation and hydration reactions, a nondimensionalisation was carried out for this model. Using results from numerical simulations, the influence of each reaction on the penetration depth was investigated in detail. Experimental data from [PVF89] was recovered.

Compared to simplified models which neglect CSH, C_2S and C_3S, it can be observed that the two silicate phases only have a small influence on the total outcome in the late stage of hydration considered here. This was found for an accelerated carbonation scenario. Further research is required with respect to natural carbonation where the effect of CSH and unhydrated constituents on the penetration depth is not a priori clear.

In general, all species compete for carbon dioxide. This slows down the carbonation of calcium hydroxide since less carbon dioxide is available to carbonation. This effect, reducing the propagation speed of the carbonation layer, was of noticable extent only for CSH. Under natural conditions, experiments suggest that the influence of the carbonation of CSH might become even smaller [cf. Cha97, e.g.] because of the worse accessibility of carbon dioxide and the possibly lesser amount of CSH available in the concrete (due to uncomplete hydration). On the other hand, for concretes with high CSH content (such as those containing blast furnace slag, fly ash, silica fume, etc.), this influence might be stronger again. Moreover, depending on the cement chemistry, several other alkaline species such as KOH, NaOH, $Mg(OH)_2$, and aluminate phases may also carbonate and, altogether, might have a noticable effect on the simulated carbonation depth.

For a large range of parameters, different reaction layers are formed associated with the several carbonation reactions. On the other hand, the hydration reactions occur fairly uniformly as long as unhydrated constituents are available. The fact that the reaction layer associated with CSH lags behind that of calcium hydroxide, which was observed experimentally by [Cha97], is also recovered in our simulations. We are not aware of experimental information about the formation of reaction zones associated with the carbonation of C_2S or C_3S.

It is well-known that the effect of moisture on the carbonation process is of considerable importance. In the model considered here, a rather simple approach was chosen. The mobile moisture influencing the rapidness of the carbonation of calcium hydroxide was modelled by a reaction-diffusion equation weakly coupled with the production term associated with the carbonation of calcium hydroxide. The effect by immobile moisture stored in the porous concrete matrix was neglected. Further research is required in order to take into account possible effects of the mobile moisture (on the diffusivities, e.g.), the immobile moisture (on the reaction rates, e.g.) as well as couplings between them. A possible better approach could be the use of double-porosity-type models. More research is required to investigate this issue.

Acknowledgments

This work has been partially supported by the Deutsche Forschungsgemeinschaft (DFG) with a grant through the special priority program SPP1122 *Prediction of the Course of Physicochemical Damage Processes Involving Mineral Materials*. We would also like to thank J. Grunewald, J. Kropp, K. Sisomphon and L. Franke for fruitful discussions.

Appendix: Dimensional parameters

We list the *standard* sets of dimensional parameters of the reference setting which we use for the numerical simulations. It refers to ordinary portland cement. There are some parameters which are definite, for instance the molecular weights of the involved species. Others are generally unknown, for instance the carbonation-reaction constants, or they strongly depend on the setting considered. Therefore, we first list all parameters in table 1. We give exact values where the parameters are definite and ranges where they are uncertain. The particular values used for the numerical simulations are given in table 2, representing an accelerated carbonation setting. Note that due to some dependencies, changing a certain parameter may imply several other changes (e.g. changing $R_{\mathrm{w/c}}$ implies a change in ϕ which, in turn, implies a different u_1^{ext} etc.).

Most of the values of the dimensional parameters can be found in the standard literature, e.g. in [Lid02]. For some specifics, we refer to [BKM03b] and [Ste00], as well as [Arf98] for values of $D_{\mathrm{H_2O}}$.

Parameter	Value	Unit	Description
$R_{\mathrm{w/c}}$	0.4 – 0.6	–	water-to-cement ratio
ϕ	0.1 – 0.6	–	concrete porosity
ϕ^{a}	0 – 1	–	volume fraction of air-filled pores
ϕ^{w}	0 – 1	–	volume fraction of water-filled pores
L	3	cm	width under consideration
$D_{\mathrm{CO_2}(g)}$	1 – 20	$\mathrm{cm}^2/\mathrm{day}$	diffusion constant for $\mathrm{CO_2}(g)$
$D_{\mathrm{CO_2}}$	10^{-6} – 10^{-2}	$\mathrm{cm}^2/\mathrm{day}$	diffusion constant for $\mathrm{CO_2}(aq)$
$D_{\mathrm{Ca(OH)_2}}$	10^{-9} – 10^{-5}	$\mathrm{cm}^2/\mathrm{day}$	diffusion constant for $\mathrm{Ca(OH)_2}(aq)$
$D_{\mathrm{H_2O}}$	10^{-3} – 10^{-1}	$\mathrm{cm}^2/\mathrm{day}$	diffusion constant for moisture
C^{Henry}	0.7 – 0.9	–	dimensionless Henry constant
C^{ex}	10^0 – 10^6	1/day	mass transfer coefficient for absorption of $\mathrm{CO_2}(g)$
$C^{\mathrm{Rob}}_{\mathrm{CO_2}(g)}$	1 – 10^5	cm/day	mass transfer coefficient for $\mathrm{CO_2}$ for exchange at the exposed boundary
$C^{\mathrm{Rob}}_{\mathrm{H_2O}}$	1 – 10^7	cm/day	mass transfer coefficient for moisture for exchange at the exposed boundary
$C^{\mathrm{reac}}_{\mathrm{Ca(OH)_2}}$	10^2 – 10^4	$\frac{\mathrm{cm}^3}{\mathrm{g}^{p+q}\mathrm{day}}$	carbonation reaction constant of $\mathrm{Ca(OH)_2}$
$C^{\mathrm{reac}}_{\mathrm{CSH}}$	10^{-1} – 10^1	$\frac{\mathrm{cm}^3}{\mathrm{g\,day}}$	carbonation reaction constant of CSH
$C^{\mathrm{reac}}_{\mathrm{C_2S}}$	10^{-1} – 10^1	$\frac{\mathrm{cm}^3}{\mathrm{g\,day}}$	carbonation reaction constant of $\mathrm{C_2S}$
$C^{\mathrm{reac}}_{\mathrm{C_3S}}$	10^{-1} – 10^1	$\frac{\mathrm{cm}^3}{\mathrm{g\,day}}$	carbonation reaction constant of $\mathrm{C_3S}$
$C^{\mathrm{hydr}}_{\mathrm{C_2S}}$	10^{-3} – 10^{-1}	$\frac{\mathrm{cm}^3}{\mathrm{g}^{p_{\mathrm{C_2S}}}\mathrm{day}}$	hydration reaction constant of $\mathrm{C_2S}$
$C^{\mathrm{hydr}}_{\mathrm{C_3S}}$	10^{-3} – 10^{-1}	$\frac{\mathrm{cm}^3}{\mathrm{g}^{p_{\mathrm{C_3S}}}\mathrm{day}}$	hydration reaction constant of $\mathrm{C_3S}$
p	1	–	exponent in carbonation reaction rate of $\mathrm{Ca(OH)_2}$
q	1	–	exponent in carbonation reaction rate of $\mathrm{Ca(OH)_2}$
$p_{\mathrm{C_2S}}$	1 – 4	–	exponent in hydration reaction rate of $\mathrm{C_2S}$
$p_{\mathrm{C_3S}}$	1 – 4	–	exponent in hydration reaction rate of $\mathrm{C_3S}$
$m_{\mathrm{CO_2}}$	44	g/mole	molecular weight of $\mathrm{CO_2}$
$m_{\mathrm{Ca(OH)_2}}$	74	g/mole	molecular weight of $\mathrm{Ca(OH)_2}$
$m_{\mathrm{H_2O}}$	18	g/mole	molecular weight of water
$m_{\mathrm{CaCO_3}}$	100	g/mole	molecular weight of $\mathrm{CaCO_3}$
m_{CSH}	342	g/mole	molecular weight of CSH
$m_{\mathrm{C_2S}}$	228	g/mole	molecular weight of $\mathrm{C_2S}$
$m_{\mathrm{C_3S}}$	172	g/mole	molecular weight of $\mathrm{C_3S}$
$\phi\phi^{\mathrm{a}}c^0_{\mathrm{CO_2}(g)}$	0	$\mathrm{g/cm}^3$	initial concentration of $\mathrm{CO_2}(g)$
$\phi\phi^{\mathrm{w}}c^0_{\mathrm{CO_2}}$	0	$\mathrm{g/cm}^3$	initial concentration of $\mathrm{CO_2}(aq)$
$\phi\phi^{\mathrm{w}}c^0_{\mathrm{Ca(OH)_2}}$	0.01 – 0.08	$\mathrm{g/cm}^3$	initial concentration of $\mathrm{Ca(OH)_2}(aq)$
ϕw^0	0.02 – 0.04	$\mathrm{g/cm}^3$	initial concentration of moisture
$\phi\phi^{\mathrm{w}}c^0_{\mathrm{CaCO_3}}$	0	$\mathrm{g/cm}^3$	initial concentration of $\mathrm{CaCO_3}$
$\phi\phi^{\mathrm{w}}c^0_{\mathrm{CSH}}$	0.01 – 0.1	$\mathrm{g/cm}^3$	initial concentration of CSH
$\phi\phi^{\mathrm{w}}c^0_{\mathrm{C_2S}}$	0.001 – 0.01	$\mathrm{g/cm}^3$	initial concentration of $\mathrm{C_2S}$
$\phi\phi^{\mathrm{w}}c^0_{\mathrm{C_3S}}$	0.001 – 0.01	$\mathrm{g/cm}^3$	initial concentration of $\mathrm{C_3S}$
$c^{\mathrm{ext}}_{\mathrm{CO_2}}$	10^{-3} – 10^{-7}	$\mathrm{g/cm}^3$	ambient concentration of $\mathrm{CO_2}(g)$
ϕw^{ext}	0.02 – 0.04	$\mathrm{g/cm}^3$	ambient concentration of moisture
a	-0.11	–	fitting parameter in sorption isotherm
b	22.7	cm^3/g	fitting parameter in sorption isotherm

Table 1: Values and ranges of dimensional parameters.

Parameter	Value	Unit
$R_{\mathrm{w/c}}$	0.5	–
ϕ	0.54	–
ϕ^{a}	0.5	–
ϕ^{w}	0.5	–
$D_{\mathrm{CO_2}(g)}$	12	$\mathrm{cm}^2/\mathrm{day}$
$D_{\mathrm{CO_2}}$	$1 \cdot 10^{-4}$	$\mathrm{cm}^2/\mathrm{day}$
$D_{\mathrm{Ca(OH)_2}}$	$1 \cdot 10^{-7}$	$\mathrm{cm}^2/\mathrm{day}$
$D_{\mathrm{H_2O}}$	$1 \cdot 10^{-2}$	$\mathrm{cm}^2/\mathrm{day}$
C^{Henry}	0.85	–
C^{ex}	$1 \cdot 10^{3}$	$1/\mathrm{day}$
$C^{\mathrm{Rob}}_{\mathrm{CO_2}(g)}$	$1 \cdot 10^{5}$	cm/day
$C^{\mathrm{Rob}}_{\mathrm{H_2O}}$	$1 \cdot 10^{7}$	cm/day
$C^{\mathrm{reac}}_{\mathrm{Ca(OH)_2}}$	450	$\frac{\mathrm{cm}^3}{\mathrm{g}^{p+q}\mathrm{day}}$
$C^{\mathrm{reac}}_{\mathrm{CSH}}$	0.25	$\frac{\mathrm{cm}^3}{\mathrm{gday}}$
$C^{\mathrm{reac}}_{\mathrm{C_2S}}$	0.18	$\frac{\mathrm{cm}^3}{\mathrm{gday}}$
$C^{\mathrm{reac}}_{\mathrm{C_3S}}$	0.14	$\frac{\mathrm{cm}^3}{\mathrm{gday}}$
$C^{\mathrm{hydr}}_{\mathrm{C_2S}}$	0.014	$\frac{\mathrm{cm}^3}{\mathrm{g}^{p_{\mathrm{C_2S}}}\mathrm{day}}$
$C^{\mathrm{hydr}}_{\mathrm{C_3S}}$	0.043	$\frac{\mathrm{cm}^3}{\mathrm{g}^{p_{\mathrm{C_3S}}}\mathrm{day}}$
$p_{\mathrm{C_2S}}$	3.1	–
$p_{\mathrm{C_3S}}$	2.65	–
$\phi\phi^{w} c^{0}_{\mathrm{Ca(OH)_2}}$	0.077	g/cm^3
ϕw^{0}	0.033	g/cm^3
$c^{\mathrm{ext}}_{\mathrm{CO_2}(g)}$	$8.7 \cdot 10^{-4}$	g/cm^3
ϕw^{ext}	0.033	g/cm^3
$\phi\phi^{\mathrm{w}} c^{0}_{\mathrm{CSH}}$	0.043	g/cm^3
$\phi\phi^{\mathrm{w}} c^{0}_{\mathrm{C_2S}}$	0.0074	g/cm^3
$\phi\phi^{\mathrm{w}} c^{0}_{\mathrm{C_3S}}$	0.0015	g/cm^3

Table 2: Specification of the values of table 1 used in the simulations.

References

[Arf98] J. Arfvidsson. *Moisture Transport in Porous Media. Modelling Based on Kirchhoff Potentials*. PhD thesis, Department of Building Technology, Building Physics, Lund University, 1998. Report TVBH-1010.

[Bie88] Th. A. Bier. *Karbonatisierung und Realkalisierung von Zementstein und Beton*. PhD thesis, University Fridericiana in Karlsruhe, Karlsruhe, 1988. Schriftenreihe des Instituts für Massivbau und Baustofftechnologie. Editors: J. Eibl, H. K. Hilsdorf.

[BKM03a] M. Böhm, J. Kropp, and A. Muntean. A two-reaction-zones moving-interface model for predicting $Ca(OH)_2$-carbonation in concrete. Berichte aus der Technomathematik 03–04, ZeTeM, University of Bremen, 2003.

[BKM03b] M. Böhm, J. Kropp, and A. Muntean. On a prediction model for concrete carbonation based on moving interfaces – interface concentrated reactions. Berichte aus der Technomathematik 03–03, ZeTeM, University of Bremen, 2003.

[Cha97] T. Chaussadent. Analyse des mécanismes de carbonatation du beton. In *AFPC-AFREM Durabilite des Betons "Méthodes recommandés pour la mesure des gradeurs associés à la durabilité"*, pages 75–86, Toulouse, France, 11–12 December 1997. INSA Génie Civil.

[Cha99] T. Chaussadent. États de lieux et réflexions sur la carbonatation du beton armé. Technical report, Laboratoire Central de Ponts et Chaussées, Paris, 1999.

[CTTJ04] J. J. Chen, J. J. Thomas, H. F. W. Taylor, and H. M. Jennings. Solubility and structure of calcium silicate hydrate. *Cement and Concrete Research*, 34:1499–1519, 2004.

[DdNC05] F. Dunstetter, M.-N. de Noirfontaine, and M. Courtial. Polymorphism of tricalcium silicate, the major compound of portland cement clinker 1. Structural data: review and unified analysis. *Cement and Concrete Research*, 2005. (in press).

[DL92] R. Dautray and J.-L. Lions. *Evolution Problems I*, volume 5 of *Mathematical analysis and numerical methods for science and technology*. Springer, 1992.

[FB90] G. F. Froment and K. B. Bischoff. *Chemical Reactor Analysis and Design*. Wiley Series in Chemical Engineering. John Wiley and Sons, 2nd edition, 1990.

[GM03] R. Grotmaack and A. Muntean. Stabilitätsanalyse eines Moving-Boundary-Modells der beschleunigten Karbonatisierung von Portlandzementen. Berichte aus der Technomathematik 03–12, ZeTeM, University of Bremen, 2003.

[Gru97] J. Grunewald. *Diffusiver und konvektiver Stoff- und Energietransport in kapillarporösen Baustoffen*. PhD thesis, Technical University of Dresden, 1997.

[Hor97] U. Hornung, editor. *Homogenization and Porous Media*. Springer, 1997.

[Hou96] Y. F. Houst. The role of moisture in the carbonation of cementious materials. *Internationale Zeitschrift für Bauinstandsetzen*, 2(1):49–66, 1996.

[HW02] Y. F. Houst and F. H. Wittmann. Depth profiles of carbonates formed during natural carbonation. *Cement and Concrete Research*, 32:1923–1930, 2002.

[IM01] T. Ishida and K. Maekawa. Modeling of pH profile in pore water based on mass transport and chemical equilibrium theory. *Concrete Library of JSCE*, 37:131–146, 2001.

[KA00] P. Knabner and L. Angermann. *Numerik partieller Differentialgleichungen. Eine anwendungsorientierte Einführung*. Springer, Berlin, 2000.

[KK01] D. A. Kulik and M. Kersten. Aqueous solubility diagrams for cementitious waste stabilization systems: II, end-member stoichiometries of ideal calcium silicate hydrate solid solutions. *J. Am. Ceram. Soc.*, 84(12):3017–3026, 2001.

[Kro95] J. Kropp. Relations between transport characteristics and durability. In J. Kropp and H. K. Hilsdorf, editors, *Performance Criteria for Concrete Durability*, RILEM Report 12, pages 97–137. E and FN Spon Editions, 1995.

[Lid02] David R. Lide, editor. *CRC Handbook of Chemistry and Physics*. CRC Press LLC, 82 edition, 2001–2002. A Ready-Reference Book of Chemical and Physical Data.

[MIK03] K. Maekawa, T. Ishida, and T. Kishi. Multi-scale modeling of concrete performance. integrated material and structural mechanics. *Journal of Advanced Concrete Technology*, 1(2):91–126, 2003. Japan Concrete Institute.

[MPMB05] S. A. Meier, M. A. Peter, A. Muntean, and M. Böhm. Modelling and simulation of concrete carbonation with internal layers. Berichte aus der Technomathematik 05-02, ZeTeM, University of Bremen, 2005.

[MS01] B. Möser and J. Stark. A new model to ordinary portland cement hydration derived by means of ESEM-FEG. In *Proceedings of the 2nd workshop "Cement and Concrete: Trends and Challenges"*, Anna Maria Island, USA, 2001.

[Mun05] A. Muntean. *Moving Carbonation Models*. PhD thesis, ZeTeM, Departement of Mathematics, University of Bremen, 2005. In preparation.

[PBK01] S. J. Preece, J. Billingham, and A. C. King. On the initial stages of cement hydration. *J. Engng. Math.*, 40:43–58, 2001.

[PVF89] V. G. Papadakis, C. G. Vayenas, and M. N. Fardis. A reaction engineering approach to the problem of concrete carbonation. *AIChE Journal*, 35:1639, 1989.

[Ram01] V. S. Ramachandran. Concrete science. In V. S. Ramachandran and J. J. Beaudoin, editors, *Handbook of Analytical Techniques in Concrete Science and Technology*, pages 1–62. Noyes Publications, 2001.

[SBK03] A. Salhan, J. Billingham, and A. C. King. The effect of a retarder on the hydration of tricacium silicate. *J. Eng. Math.*, 45:367–377, 2003.

[SD96] F. Schmidt-Döhl. Ein modell zur berechnung von kombibierten chemischen reaktions- und transportprozessen und seine anwendung auf die korrosion mineralischer baustoffe. Technical Report 125, Institut für Baustoffe, Massivbau und Brandschutz, TU Braunschweig, 1996.

[SDA02] A. Steffens, D. Dinkler, and H. Ahrens. Modeling carbonation for corrosion risk prediction of concrete structures. *Cement and Concrete Research*, 32:935–941, 2002.

[Sis04] K. Sisomphon. *Influence of Pozzolanic Material Additions on the Development of the Alkalinity and the Carbonation Behaviour of Composite Cement Pastes and Concretes*. PhD thesis, TU Hamburg-Harburg, 2004.

[SSV93] A. V. Saetta, B. A. Schrefler, and R. V. Vitaliani. The carbonation of concrete and the mechanism of moisture, heat and carbon dioxide flow through porous materials. *Cement and Concrete Research*, 23(4):761–772, 1993.

[SSV95] A. V. Saetta, B. A. Schrefler, and R. V. Vitaliani. 2D model for carbonation and moisture/heat flow in porous materials. *Cement and Concrete Research*, 25(8):1703–1712, 1995.

[Ste00] A. Steffens. *Modellierung von Karbonatisierung und Chloridbindung zur numerischen Analyse der Korrosionsgefährdung der Betonbewehrung.* PhD thesis, Institute for Statics, Technical University Braunschweig, 2000.

[SV04] A. V. Saetta and R. V. Vitaliani. Experimental investigation and numerical modeling of carbonation process in reinforced concrete structures. Part I: Theoretical formulation. *Cement and Concrete Research*, 34(4):571–579, 2004.

[Tay97] H. F. W. Taylor. *Cement Chemistry.* Thomas Telford Publishing, London, 1997.

Berichte aus der Technomathematik ISSN 1435-7968

http://www.math.uni-bremen.de/zetem/berichte.html

— Vertrieb durch den Autor —

Reports **Stand: 20. April 2005**

98–01. Peter Benner, Heike Faßbender:
An Implicitly Restarted Symplectic Lanczos Method for the Symplectic Eigenvalue Problem, Juli 1998.

98–02. Heike Faßbender:
Sliding Window Schemes for Discrete Least-Squares Approximation by Trigonometric Polynomials, Juli 1998.

98–03. Peter Benner, Maribel Castillo, Enrique S. Quintana-Ortí:
Parallel Partial Stabilizing Algorithms for Large Linear Control Systems, Juli 1998.

98–04. Peter Benner:
Computational Methods for Linear–Quadratic Optimization, August 1998.

98–05. Peter Benner, Ralph Byers, Enrique S. Quintana-Ortí, Gregorio Quintana-Ortí:
Solving Algebraic Riccati Equations on Parallel Computers Using Newton's Method with Exact Line Search, August 1998.

98–06. Lars Grüne, Fabian Wirth:
On the rate of convergence of infinite horizon discounted optimal value functions, November 1998.

98–07. Peter Benner, Volker Mehrmann, Hongguo Xu:
A Note on the Numerical Solution of Complex Hamiltonian and Skew-Hamiltonian Eigenvalue Problems, November 1998.

98–08. Eberhard Bänsch, Burkhard Höhn:
Numerical simulation of a silicon floating zone with a free capillary surface, Dezember 1998.

99–01. Heike Faßbender:
The Parameterized SR Algorithm for Symplectic (Butterfly) Matrices, Februar 1999.

99–02. Heike Faßbender:
Error Analysis of the symplectic Lanczos Method for the symplectic Eigenvalue Problem, März 1999.

99–03. Eberhard Bänsch, Alfred Schmidt:
Simulation of dendritic crystal growth with thermal convection, März 1999.

99–04. Eberhard Bänsch:
Finite element discretization of the Navier-Stokes equations with a free capillary surface, März 1999.

99–05. Peter Benner:
Mathematik in der Berufspraxis, Juli 1999.

99–06. Andrew D.B. Paice, Fabian R. Wirth:
Robustness of nonlinear systems and their domains of attraction, August 1999.

99–07. Peter Benner, Enrique S. Quintana-Ortí, Gregorio Quintana-Ortí:
Balanced Truncation Model Reduction of Large-Scale Dense Systems on Parallel Computers, September 1999.

99–08. Ronald Stöver:
Collocation methods for solving linear differential-algebraic boundary value problems, September 1999.

99–09. Huseyin Akcay:
Modelling with Orthonormal Basis Functions, September 1999.

99–10. Heike Faßbender, D. Steven Mackey, Niloufer Mackey:
Hamilton and Jacobi come full circle: Jacobi algorithms for structured Hamiltonian eigenproblems, Oktober 1999.

99–11. Peter Benner, Vincente Hernández, Antonio Pastor:
On the Kleinman Iteration for Nonstabilizable System, Oktober 1999.

99–12. Peter Benner, Heike Faßbender:
A Hybrid Method for the Numerical Solution of Discrete-Time Algebraic Riccati Equations, November 1999.

99–13. Peter Benner, Enrique S. Quintana-Ortí, Gregorio Quintana-Ortí:
Numerical Solution of Schur Stable Linear Matrix Equations on Multicomputers, November 1999.

99–14. Eberhard Bänsch, Karol Mikula:
Adaptivity in 3D Image Processing, Dezember 1999.

00–01. Peter Benner, Volker Mehrmann, Hongguo Xu:
Perturbation Analysis for the Eigenvalue Problem of a Formal Product of Matrices, Januar 2000.

00–02. Ziping Huang:
Finite Element Method for Mixed Problems with Penalty, Januar 2000.

00–03. Gianfrancesco Martinico:
Recursive mesh refinement in 3D, Februar 2000.

00–04. Eberhard Bänsch, Christoph Egbers, Oliver Meincke, Nicoleta Scurtu:
Taylor-Couette System with Asymmetric Boundary Conditions, Februar 2000.

00–05. Peter Benner:
Symplectic Balancing of Hamiltonian Matrices, Februar 2000.

00–06. Fabio Camilli, Lars Grüne, Fabian Wirth:
A regularization of Zubov's equation for robust domains of attraction, März 2000.

00–07. Michael Wolff, Eberhard Bänsch, Michael Böhm, Dominic Davis:
Modellierung der Abkühlung von Stahlbrammen, März 2000.

00–08. Stephan Dahlke, Peter Maaß, Gerd Teschke:
Interpolating Scaling Functions with Duals, April 2000.

00–09. Jochen Behrens, Fabian Wirth:
A globalization procedure for locally stabilizing controllers, Mai 2000.

00–10. Peter Maaß, Gerd Teschke, Werner Willmann, Günter Wollmann:
Detection and Classification of Material Attributes – A Practical Application of Wavelet Analysis, Mai 2000.

00–11. Stefan Boschert, Alfred Schmidt, Kunibert G. Siebert, Eberhard Bänsch, Klaus-Werner Benz, Gerhard Dziuk, Thomas Kaiser:
Simulation of Industrial Crystal Growth by the Vertical Bridgman Method, Mai 2000.

00–12. Volker Lehmann, Gerd Teschke:
Wavelet Based Methods for Improved Wind Profiler Signal Processing, Mai 2000.

00–13. Stephan Dahlke, Peter Maass:
A Note on Interpolating Scaling Functions, August 2000.

00–14. Ronny Ramlau, Rolf Clackdoyle, Frédéric Noo, Girish Bal:
Accurate Attenuation Correction in SPECT Imaging using Optimization of Bilinear Functions and Assuming an Unknown Spatially-Varying Attenuation Distribution, September 2000.

00–15. Peter Kunkel, Ronald Stöver:
Symmetric collocation methods for linear differential-algebraic boundary value problems, September 2000.

00–16. Fabian Wirth:
The generalized spectral radius and extremal norms, Oktober 2000.

00–17. Frank Stenger, Ahmad Reza Naghsh-Nilchi, Jenny Niebsch, Ronny Ramlau:
A unified approach to the approximate solution of PDE, November 2000.

00–18. Peter Benner, Enrique S. Quintana-Ortí, Gregorio Quintana-Ortí:
Parallel algorithms for model reduction of discrete–time systems, Dezember 2000.

00–19. Ronny Ramlau:
A steepest descent algorithm for the global minimization of Tikhonov–Phillips functional, Dezember 2000.

01–01. Efficient methods in hyperthermia treatment planning:
Torsten Köhler, Peter Maass, Peter Wust, Martin Seebass, Januar 2001.

01–02. Parallel Algorithms for LQ Optimal Control of Discrete-Time Periodic Linear Systems:
Peter Benner, Ralph Byers, Rafael Mayo, Enrique S. Quintana-Ortí, Vicente Hernández, Februar 2001.

01–03. Peter Benner, Enrique S. Quintana-Ortí, Gregorio Quintana-Ortí:
Efficient Numerical Algorithms for Balanced Stochastic Truncation, März 2001.

01–04. Peter Benner, Maribel Castillo, Enrique S. Quintana-Ortí:
Partial Stabilization of Large-Scale Discrete-Time Linear Control Systems, März 2001.

01–05. Stephan Dahlke:
Besov Regularity for Edge Singularities in Polyhedral Domains, Mai 2001.

01–06. Fabian Wirth:
A linearization principle for robustness with respect to time-varying perturbations, Mai 2001.

01–07. Stephan Dahlke, Wolfgang Dahmen, Karsten Urban:
Adaptive Wavelet Methods for Saddle Point Problems - Optimal Convergence Rates, Juli 2001.

01–08. Ronny Ramlau:
Morozov's Discrepancy Principle for Tikhonov regularization of nonlinear operators, Juli 2001.

01–09. Michael Wolff:
Einführung des Drucks für die instationären Stokes–Gleichungen mittels der Methode von Kaplan, Juli 2001.

01–10. Stephan Dahlke, Peter Maaß, Gerd Teschke:
Reconstruction of Reflectivity Desities by Wavelet Transforms, August 2001.

01–11. Stephan Dahlke:
Besov Regularity for the Neumann Problem, August 2001.

01–12. Bernard Haasdonk, Mario Ohlberger, Martin Rumpf, Alfred Schmidt, Kunibert G. Siebert:
h–p–Multiresolution Visualization of Adaptive Finite Element Simulations, Oktober 2001.

01–13. Stephan Dahlke, Gabriele Steidl, Gerd Teschke:
Coorbit Spaces and Banach Frames on Homogeneous Spaces with Applications to Analyzing Functions on Spheres, August 2001.

02–01. Michael Wolff, Michael Böhm:
Zur Modellierung der Thermoelasto-Plastizität mit Phasenumwandlungen bei Stählen sowie der Umwandlungsplastizität, Februar 2002.

02–02. Stephan Dahlke, Peter Maaß:
An Outline of Adaptive Wavelet Galerkin Methods for Tikhonov Regularization of Inverse Parabolic Problems, April 2002.

02–03. Alfred Schmidt:
A Multi-Mesh Finite Element Method for Phase Field Simulations, April 2002.

02–04. Sergey N. Dachkovski, Michael Böhm:
A Note on Finite Thermoplasticity with Phase Changes, Juli 2002.

02–05. Michael Wolff, Michael Böhm:
Phasenumwandlungen und Umwandlungsplastizität bei Stählen im Konzept der Thermoelasto-Plastizität, Juli 2002.

02–06. Gerd Teschke:
Construction of Generalized Uncertainty Principles and Wavelets in Anisotropic Sobolev Spaces, August 2002.

02–07. Ronny Ramlau:
TIGRA – an iterative algorithm for regularizing nonlinear ill–posed problems, August 2002.

02–08. Michael Lukaschewitsch, Peter Maaß, Michael Pidcock:
Tikhonov regularization for Electrical Impedance Tomography on unbounded domains, Oktober 2002.

02–09. Volker Dicken, Peter Maaß, Ingo Menz, Jenny Niebsch, Ronny Ramlau:
Inverse Unwuchtidentifikation an Flugtriebwerken mit Quetschöldämpfern, Oktober 2002.

02–10. Torsten Köhler, Peter Maaß, Jan Kalden:
Time-series forecasting for total volume data and charge back data, November 2002.

02–11. Angelika Bunse-Gerstner:
A Short Introduction to Iterative Methods for Large Linear Systems, November 2002.

02–12. Peter Kunkel, Volker Mehrmann, Ronald Stöver:
Symmetric Collocation for Unstructured Nonlinear Differential-Algebraic Equations of Arbitrary Index, November 2002.

02–13. Michael Wolff:
Ringvorlesung: Distortion Engineering 2
Kontinuumsmechanische Modellierung des Materialverhaltens von Stahl unter Berücksichtigung von Phasenumwandlungen, Dezember 2002.

02–14. Michael Böhm, Martin Hunkel, Alfred Schmidt, Michael Wolff:
Evaluation of various phase-transition models for 100Cr6 for application in commercial FEM programs, Dezember 2002.

03–01. Michael Wolff, Michael Böhm, Serguei Dachkovski:
Volumenanteile versus Massenanteile - der Dilatometerversuch aus der Sicht der Kontinuumsmechanik, Januar 2003.

03–02. Daniel Kessler, Ricardo H. Nochetto, Alfred Schmidt:
A posteriori error control for the Allen-Cahn Problem: circumventing Gronwall's inequality, März 2003.

03–03. Michael Böhm, Jörg Kropp, Adrian Muntean:
On a Prediction Model for Concrete Carbonation based on Moving Interfaces - Interface concentrated Reactions, April 2003.

03–04. Michael Böhm, Jörg Kropp, Adrian Muntean:
A Two-Reaction-Zones Moving-Interface Model for Predicting $Ca(OH)_2$ Carbonation in Concrete, April 2003.

03–05. Vladimir L. Kharitonov, Diederich Hinrichsen:
Exponential estimates for time delay systems, May 2003.

03–06. Michael Wolff, Michael Böhm, Serguei Dachkovski, Günther Löwisch:
Zur makroskopischen Modellierung von spannungsabhängigem Umwandlungsverhalten und Umwandlungsplastizität bei Stählen und ihrer experimentellen Untersuchung in einfachen Versuchen, Juli 2003.

03–07. Serguei Dachkovski, Michael Böhm, Alfred Schmidt, Michael Wolff:
Comparison of several kinetic equations for pearlite transformation in 100Cr6 steel,
Juli 2003.

03–08. Volker Dicken, Peter Maass, Ingo Menz, Jenny Niebsch, Ronny Ramlau:
Nonlinear Inverse Unbalance Reconstruction in Rotor dynamics,
Juli 2003.

03–09. Michael Böhm, Serguei Dachkovski, Martin Hunkel, Thomas Lübben, Michael Wolff:
Übersicht über einige makroskopische Modelle für Phasenumwandlungen im Stahl,
Juli 2003.

03–10. Michael Wolff, Friedhelm Frerichs, Bettina Suhr:
Vorstudie für einen Bauteilversuch zur Umwandlungsplastizität bei der perlitischen Umwandlung des Stahls 100 Cr6,
August 2003.

03–11. Michael Wolff, Bettina Suhr:
Zum Vergleich von Massen- und Volumenanteilen bei der perlitischen Umwandlung der Stähle 100Cr6 und C80,
September 2003.

03–12. Rike Grotmaack, Adrian Muntean:
Stabilitätsanalyse eines Moving-Boundary-Modells der beschleunigten Karbonatisierung von Portlandzementen,
September 2003.

03–13. Alfred Schmidt, Michael Wolff, Michael Böhm:
Numerische Untersuchungen für ein Modell des Materialverhaltens mit Umwandlungsplastizität und Phasenumwandlungen beim Stahl 100Cr6 (Teil 1),
September 2003.

04–01. Liliana Cruz Martin, Gerd Teschke:
A new method to reconstruct radar reflectivities and Doppler information,
Januar 2004.

04–02. Ingrid Daubechies, Gerd Teschke:
Wavelet based image decomposition by variational functionals,
Januar 2004.

04–03. N. Guglielmi, F. Wirth, M. Zennaro:
Complex polytope extremality results for families of matrices,
März 2004.

04–04. I. Daubechies, G. Teschke:
Variational image restoration by means of wavelets: simultaneous decomposition, deblurring and denoising,
April 2004.

04–05. V.L. Kharitonov, E. Plischke:
Lyapunov matrices for time-delay systems,
April 2004.

04–06. Ronny Ramlau:
On the use of fixed point iterations for the regularization of nonlinear ill-posed problems,
Juni 2004.

04–07. Christof Büskens, Matthias Knauer:
Higher Order Real-Time Approximations In Optimal Control of Multibody-Systems For Industrial Robots,
August 2004.

04–08. Christof Büskens, Roland Griesse:
Computational Parametric Sensitivity Analysis of Perturbed PDE Optimal Control Problems with State and Control Constraints,
August 2004.

04–09. Christof Büskens:
Higher Order Real-Time Approximations of Perturbed Control Constrainted PDE Optimal Control Problems ,
August 2004.

04–10. Christof Büskens, Matthias Gerdts:
Differentiability of Consistency Functions,
August 2004.

04–11. Robert Baier, Christof Büskens, Ilyes Aïssa Chama, Matthias Gerdts:
Approximation of Reachable Sets by Direct Solution Methods of Optimal Control Problems,
August 2004.

04–12. J. Soares, G. Teschke, M. Zhariy:
A Wavelet Regularization for Nonlinear Diffusion Equations,
September 2004.

05–01. Alfred Schmidt, Adrian Muntean, Michael Böhm:
Numerical experiments with Self-Adaptive Finite Element Simulations in 2D for the Carbonation of Concrete,
April 2005.

05–02. Sebastian A. Meier, Malte A. Peter, Adrian Muntean, Michael Böhm:
Modelling and simulation of concrete carbonation with internal layers,
April 2005.

05–03. Malte A. Peter, Adrian Muntean, Sebastian A. Meier, Michael Böhm:
Modelling and simulation of concrete carbonation: competition of several carbonation reactions,
April 2005.